SOLAR FLARE HARD X-RAY OBSERVATIONS

BRIAN R. DENNIS

Solar Physics Branch, Laboratory for Astronomy and Solar Physics, NASA-Goddard Space Flight Center, Greenbelt, MD 20771, U.S.A.

(Received 16 February, 1988)

Abstract. Recent hard X-ray observations of solar flares are reviewed with emphasis on results obtained with instruments on the Solar Maximum Mission satellite. Flares with three different sets of characteristics, designated as Type A, Type B, and Type C, are discussed and hard X-ray temporal, spatial, spectral, and polarization measurements are reviewed in this framework. Coincident observations are reviewed at other wavelengths including the UV, microwaves, and soft X-rays, with discussions of their interpretations. In conclusion, a brief outline is presented of the potential of future hard X-ray observations with sub-second time resolution, arcsecond spatial resolution, and keV energy resolution, and polarization measurements at the few percent level up to 100 keV.

1. Introduction

A strong case can be made that future hard X-ray observations will be pivotal in unraveling the fundamental mysteries of solar flares. Hard X-rays can provide us with the most important information required for understanding the energy release process and the mechanism or mechanisms by which particles are energized during a flare.

This paper is a review of some of the more recent results on solar hard X-ray bursts with particular emphasis on observations made with instruments on the Solar Maximum Mission (SMM). The energy range covered is from below 20 keV to above 300 keV with a discussion of the spatial, spectral, temporal, and polarization information that has been obtained over the last solar maximum. Coincident observations at other wavelengths are also discussed. An attempt is made to show how these results can be interpreted and how future observations with increased sensitivity and improved spatial and spectral resolution may answer some of the primary questions concerning energy release and particle acceleration. This review should be read as an update of an earlier paper on the same subject (Dennis, 1985). Other recent reviews of all aspects of the flare phenomenon can be found in the Centennial edition of *Solar Physics* (Vol. 100, 1985) and in the *Proceedings of the SMM Workshops* (Kundu and Woodgate, 1986). A comprehensive review of Hinotori results is given by Tanaka (1987).

The hard X-ray emission is generally agreed to be electron-ion bremsstrahlung although the recent papers by Simnett (1986) and Heristchi (1986) have reopened the question of whether it is the electrons or the ions (mainly protons) that are the primary high-energy particles (see below). In this paper, we assume that the electrons are the high-energy particles and that the hard X-ray emission derives its importance from the fact that, along with radio and microwave emission, it gives us the most direct informa-

Solar Physics **118** (1988) 49–94.

tion about the high-energy electrons produced in a flare. Since it appears that these electrons contain a significant amount of the total energy released in a flare and since they are one of the primary products of the energy release process, it is of crucial importance to determine their spatial, spectral, and temporal evolution as accurately as possible during a flare.

Although only a small fraction of the electron energy appears as bremsstrahlung (~ 1 part in 10^5), the X-rays begin to be produced as soon as the electrons are energized. Consequently, the X-rays can tell us about the earliest possible time after the flare energy is released, before the information has become degraded by the inevitable increase in entropy resulting from thermalization and other relaxation processes.

Clearly, it is also vital to determine the conditions at and around the energy release site, the magnetic field configuration, and the parameters of the plasma in the region before, during, and after the flare. The information cannot be determined from the hard X-ray observations alone and coincident observations of other emissions are required. In particular, the radio emission from energetic electrons provides unique information on the magnetic field, and soft X-ray, EUV, UV, and optical emissions provide information on the temperature, density, and velocity distributions of the thermal source. Another important objective of the observations of the thermal plasma is to determine what fraction of the heating is produced directly in the energy release process itself and what fraction is the consequence of the aforementioned increase in entropy.

This paper is a review of the current state of our knowledge of the hard X-ray emission and of the energetic particles that produce it. Coincident observations of other emissions – radio, soft X-ray, UV, Hα – are presented with emphasis on the insight into the flare processes gained by the joint analysis of these different data sets. The potential for advances from possible future observations is also discussed.

2. Flare Classification

Following Dennis (1985), I will again use the scheme first proposed by Tanaka (1983) and expanded by Tsuneta (1983) and Tanaka (1987) for grouping flares according to their combined properties, particularly their hard X-ray temporal, spectral, and spatial characteristics. Flares with three different sets of hard X-ray characteristics have been identified as follows:

Type A or Hot Thermal Flares:

Temporal: gradual rise and fall of hard X-ray emission at energies below ~ 40 keV; weak impulsive emission at higher energies;

Spectral: thermal fit below 40 keV with temperatures of $3\text{–}4 \times 10^7$ K, very steep spectra above 40 keV with power-law index $\gamma \gtrsim 7$;

Spatial: compact (< 5000 km).

Type B or Impulsive Flares:

Temporal: typical impulsive hard X-ray spikes with variability on time-scales of seconds;

Spectral: soft spectrum on the rise becoming harder at the peak and softer again on the decay; often exponential or broken power-law on the rise and at the peak, changing to a single power law on the decay;

Spatial: emission from low altitude including footpoints at the peak, evolving to a more compact source at higher altitude later in flare.

Type C or Gradual-Hard Flare:

Temporal: gradually varying hard X-ray emission on time scales of minutes sometimes lasting for 30 min or longer;

Spectral: spectrum above ~ 50 keV hardens with time with γ decreasing monotonically from $\gtrsim 5$ early in the flare to $\lesssim 2$ later in the flare after the peak;

Spatial: the source is located at high altitudes of $\gtrsim 4 \times 10^4$ km.

Most flares appear to be type B or, at least, flares with type B characteristics dominate. The relative numbers of flares of different types can be seen from the analysis of ~ 400 flares presented by Kosugi, Dennis, and Kai (1988). They found that 13 of these flares were gradual, 3 were thermal, 62 were associated with microwave gradual rise and fall (GRF) events, and most of the remaining 338 were impulsive. Most of the SMM effort has gone into understanding the more numerous impulsive flares. These may be more demanding theoretically in terms of the rate of energy release. The popular flare models are geared to releasing energy impulsively in low-lying coronal magnetic loops on time-scales of seconds, characteristics of type B events. Similarly, many of the coincident observations that have been so revealing when analyzed jointly with the hard X-rays have been of impulsive phenomena.

In comparison, relatively little work has been done on the gradual energy release at altitudes in excess of 40000 km in the corona and on time-scales of minutes. This situation is not surprising given the relative frequency of the different types of events but it must be remembered that some of the most intense flares show type C characteristics. It becomes confusing and misleading when attempts are made to apply models for type B flares to the large gradual events. It seems likely that entirely different models will be required for the different flare types with different physical processes involved. Alternatively, any comprehensive flare model must allow the possibility of at least two different flare types and different phases within the same flare.

This scheme has been criticized when it has been used to classify flares since some flares show characteristics of more than one type. De Jager and Švestka (1985) have discussed flares that have characteristics of both type B and C. Cliver *et al.* (1986a, b) show that many type C flares are preceded, sometimes by as much as 60 min, by an apparently normal type B flare.

Nitta, Kiplinger, and Kai (1988) suggest that a well observed flare that occurred on 3 February, 1982 shows clear evidence of type B and C characteristics. The event was imaged with the Solar X-Ray Telescope (SXT) on Hinotori at higher energies (~ 30 keV) than for most of the previously published Hinotori results. It was also observed with the Hard X-ray Monitor spectrometer (HXM) on Hinotori, the Hard X-Ray Burst Spectrometer (HXRBS) on SMM, the Nobeyama interferometer at

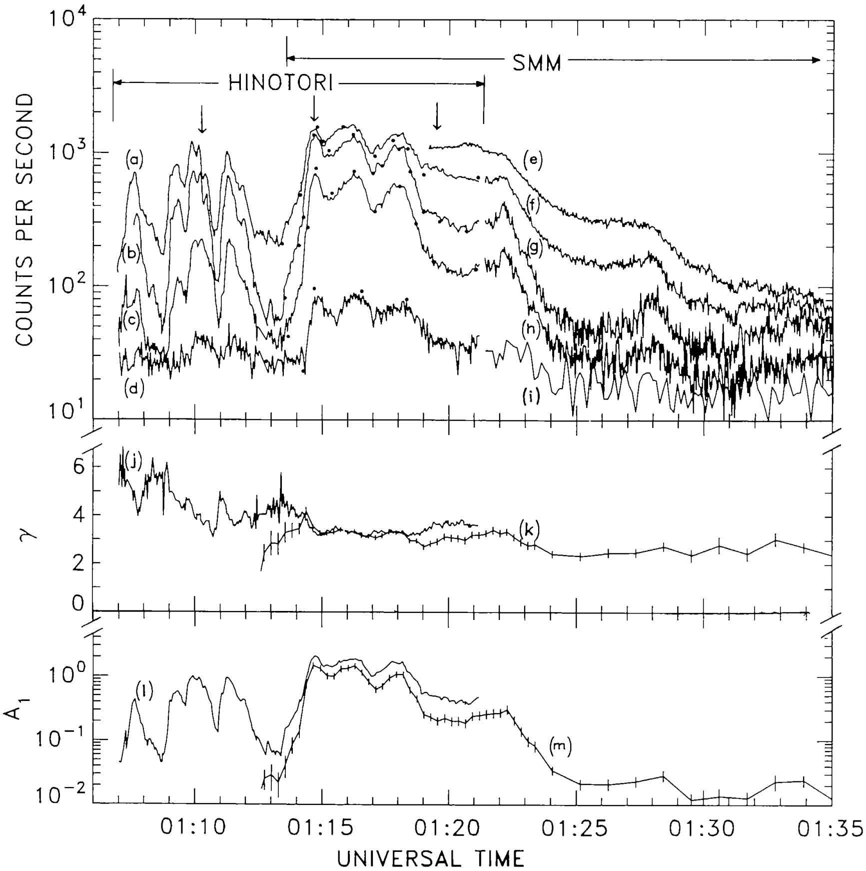

Fig. 1. Time profiles of the hard X-ray emission and the power-law spectral parameters γ and A_1 for an event on 3 February, 1982 (from Nitta, Kiplinger, and Kai, 1988). Hinotori's HXM data are shown before and HXRBS data after 01:21 UT. The nominal energy bands are (a) 28–38, (b) 38–67, (c) 67–159, and (d) 159–375 keV for HXM and (e) 31–36, (f) 36–61, (g) 61–87, (h) 87–141, and (i) 260–360 keV for HXRBS.

17 GHz, and the Mitaka optical telescope in Hα. The time profile of this event is shown in Figure 1 together with the spectral parameters for a power-law fit to the HXM and HXRBS data. The characteristic type B soft-hard-soft spectral evolution can be seen during the early impulsive phase, e.g., for the peak at 01:07:35 UT, although, in this case, the hardest spectrum occurred $\sim$5 s after the peak. The type C characteristic of spectral hardening on the decay of the more gradually varying emission is evident both in Figure 1 after 01:22 UT and, at energies above $\sim$60 keV, in the four spectra plotted in Figure 2. The impression that a type B phase is followed by a type C phase is further enhanced by the appearance of two resolved bright patches during the impulsive phase in the $\sim$30 keV X-ray images shown in Figure 3. The two bright patches visible in Figure 3(c) taken at 01:10:30 UT are located on the two brightest Hα ribbons visible in the Mitaka photographs. The X-ray images at lower energies show a source between the two hard X-ray patches suggesting that the hard X-rays are from the footpoints while the soft X-rays are from a thermal plasma filling the loops.

To further confuse the distinction between type B and C flares, the X-ray spectral hardening typical of type C flares also seems to occur at energies above $\sim$50 keV on

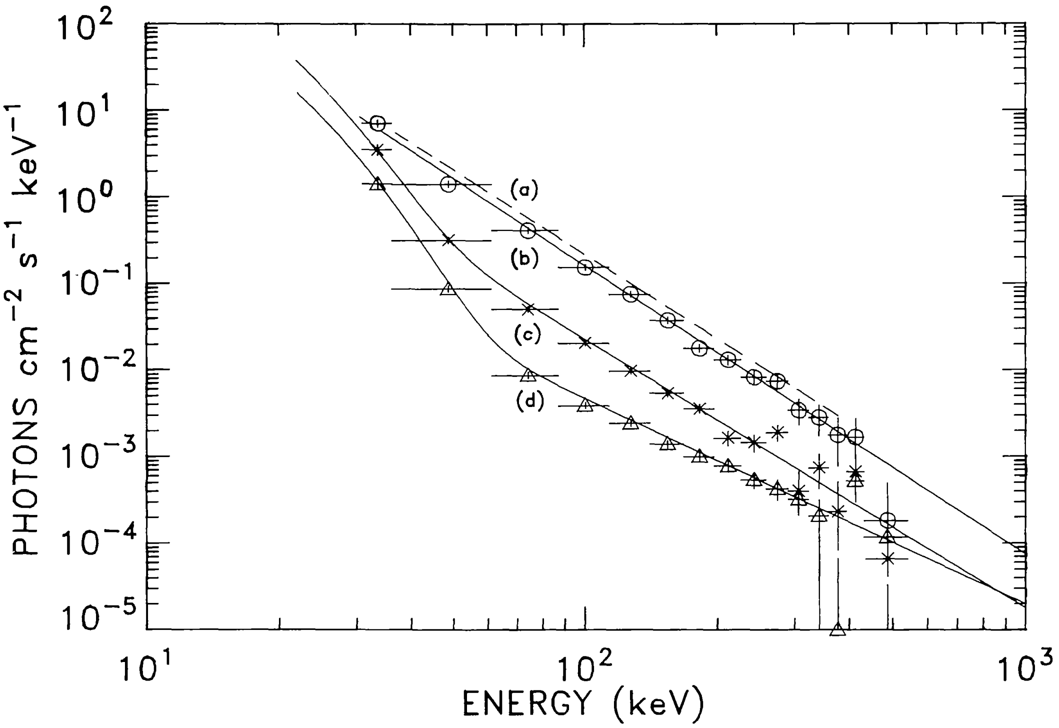

Fig. 2. HXRBS hard X-ray spectra at 01:14:43, 091:22:34, and 01:24 UT for the event shown in Figure 1 (from Nitta, Kiplinger, and Kai, 1988). The dashed curve shows the corresponding HXM spectrum obtained at 01:14:43 UT.

the decay of some impulsive events (Crannell *et al.*, 1978; Dennis, Frost, and Orwig, 1981; Starr *et al.*, 1987). Kosugi and Kiplinger (1987) have found an event with multiple impulsive spikes, some of which show the soft-hard-soft spectral evolution typical of type B flares but others that show the soft-hard-harder evolution of type C flares.

In spite of the difficulties with the separation of flares into three types – A, B, and C – this scheme does serve to clarify the distinctive properties of many flares and provides a valuable basis for identifying the common characteristics that are most likely to reveal different physical processes occurring in the different types of flares. This particular scheme has the advantage that different physical processes may well be involved in the three different flare types or at least different processes may dominate. For example, in type A flares, the energy release appears to result primarily in heating to $\lesssim 3 \times 10^7$ K with little nonthermal particle acceleration. This is possibly because of a higher density at the energy release site. In type B flares, particle acceleration is certainly more important than in type A flares although heating to $\gtrsim 10^8$ K could still explain many of the observations. In type C flares, continuous particle acceleration appears to occur at high altitudes, where the density and magnetic field must be much lower than for the low altitude type A and B flares.

It is interesting to note that most if not all type C flares are accompanied by coronal mass ejections (Cliver *et al.*, 1986a, b) although CMEs do occur with other types of flares too. It is not clear what the connection is between the flare and the CME but extrapolation of the altitude vs time plots for the CMEs back to zero altitude shows in

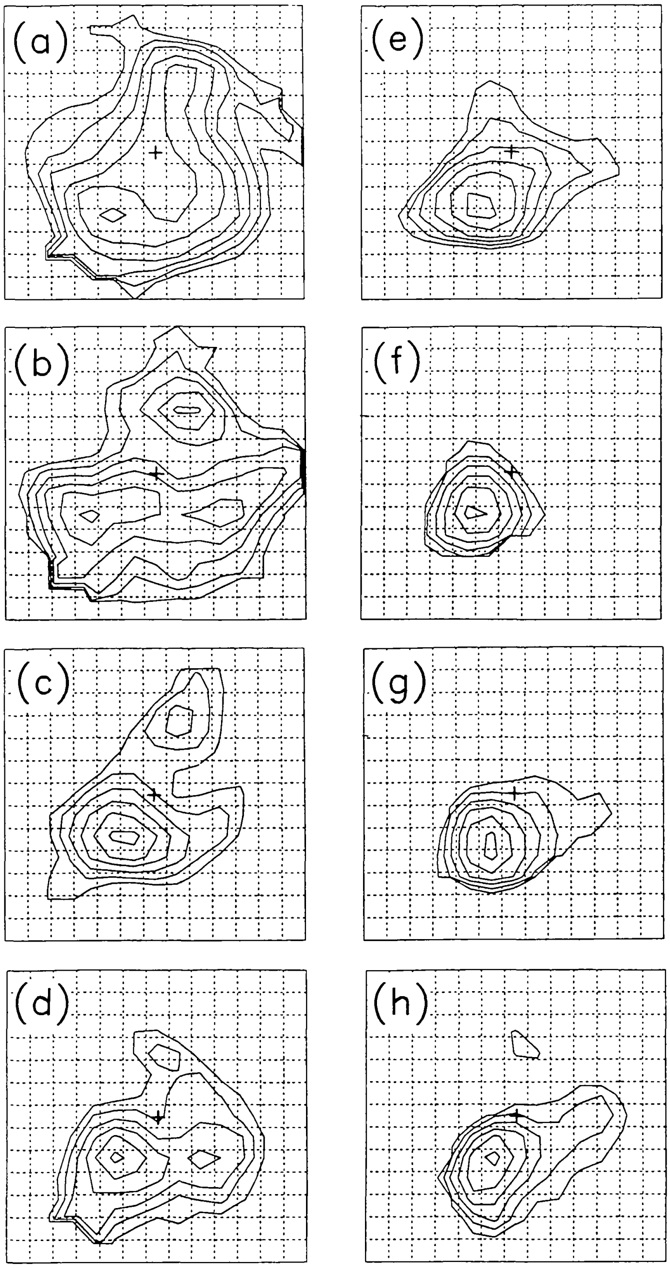

Fig. 3. Hard X-ray images obtained with SXT-2 on Hinotori in the nominal energy band of 27–54 keV at different times during the event on 3 February, 1982 shown in Figure 1 (from Nitta, Kiplinger, and Kai, 1988). Images (a) to (d) are for the impulsive bursts between 01:09:20 and 01:10:30 UT and (e) to (h) are for the main gradual peak between 01:14:20 and 01:15:20 UT.

many cases that the CME must have lifted off well before the start of the hard X-ray burst. The only emission detected at the time of the lift-off is usually relatively weak soft X-rays (Simnett and Harrison, 1985; Harrison *et al.*, 1985; Harrison, 1986). This conclusion is supported by Kahler *et al.* (1988), who note that filament eruptions also begin before the onset of the impulsive phase and evolve smoothly through the impulsive phase. This surprising result suggests that the flare is a consequence of the associated filament eruption and CME rather than that the eruption and CME are consequences of the flare.

3. Temporal Observations

3.1. Preflash phase

A distinct preflash phase had been discussed by Benz *et al.* (1983) based on hard X-ray and decimetric radio observations prior to the flash phase in 7 of 45 flares studied. They note that in these 7 events, even before the 'preflash' phase, there is an earlier 'preflare' phase in which decimetric (DCIM) and soft X-ray emission is observed. Three examples

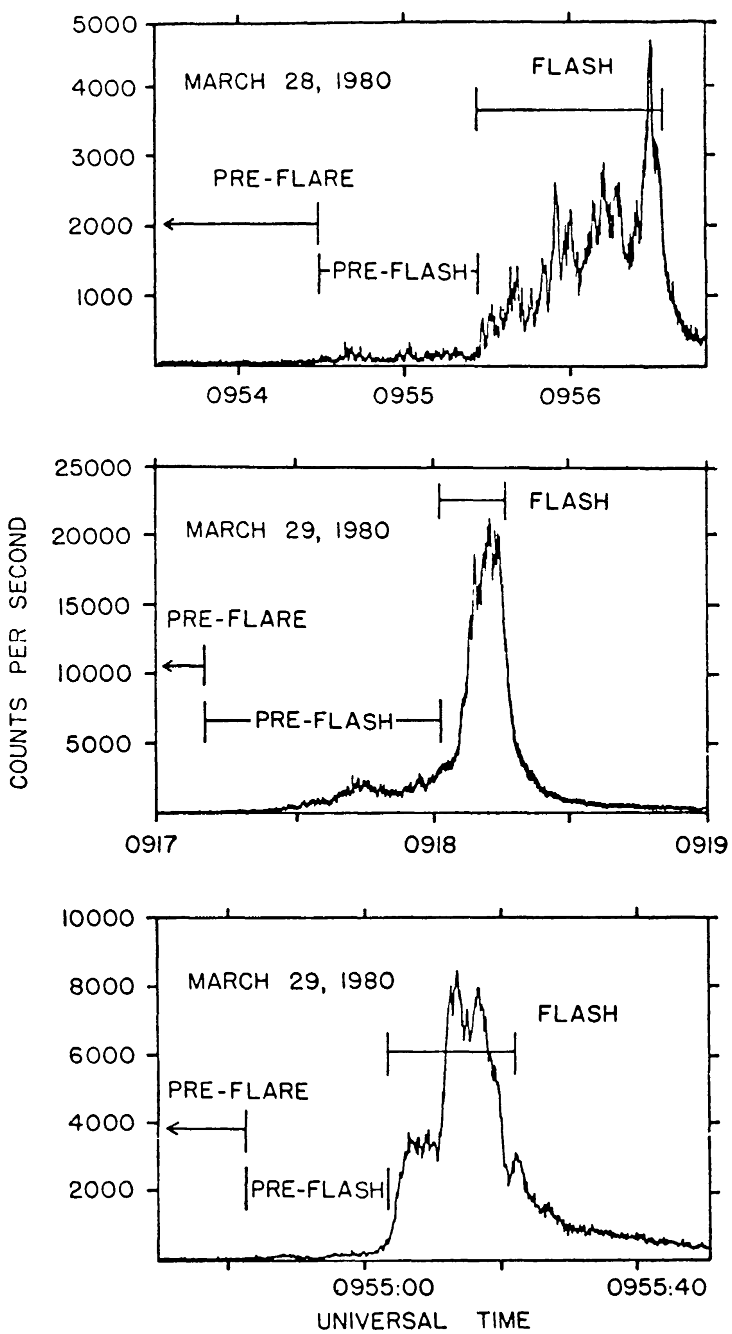

Fig. 4. Hard X-ray emission of three events observed with HXRBS in the energy range from 26 to 461 keV with a time resolution of 0.128 s. The various phases are indicated for each event (from Benz *et al.*, 1983).

of such events are shown in Figure 4. During the preflash phase, hard X-ray spikes and type III radio bursts appear, some of them apparently correlated, with the type III bursts delayed by 0.1–1.8 s (see Figure 5 and also Dennis *et al.*, 1984). The locations of the type III's at 168 MHz may be different from that observed later during the flash phase (Raoult *et al.*, 1985). In addition to the rapid hard X-ray spectral hardening at the start of the flash phase, they also note the disappearance of the DCIM emission at this time.

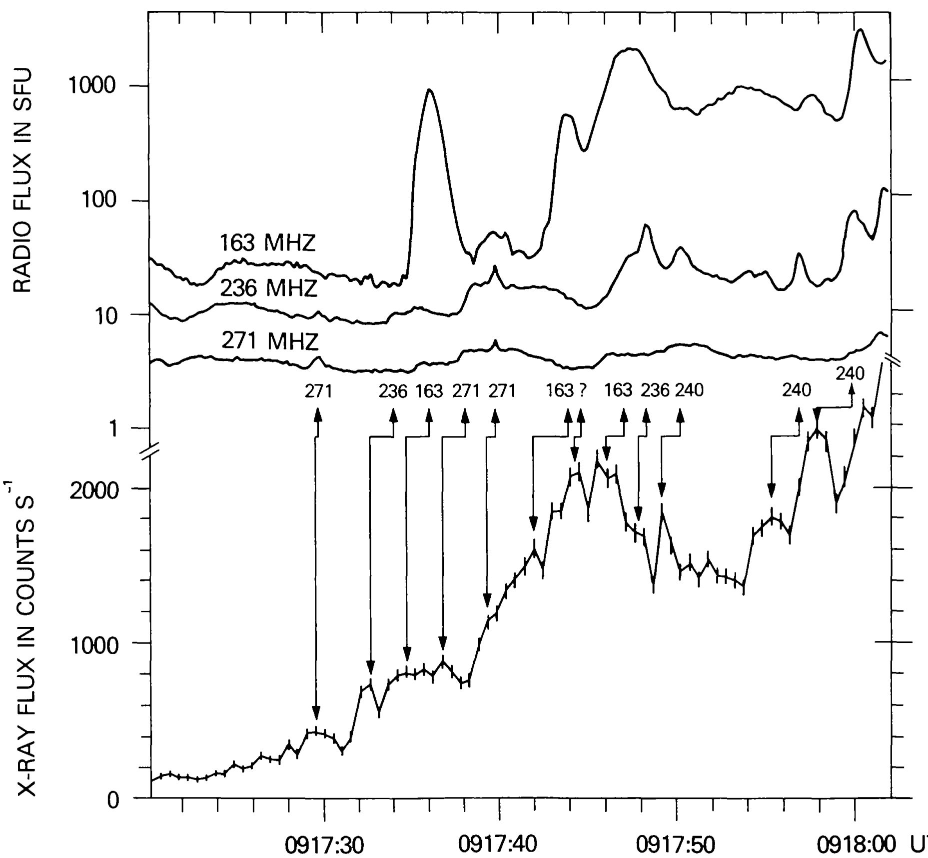

Fig. 5. Radio flux at 163, 236, and 271 MHz plotted on the same time scale as the 26 to 461 X-ray flux for the flare on 7 March, 1980 at 09:18 UT. Each double arrow indicates a significant X-ray peak or shoulder and the first, possibly associated, type III burst following it. The numbers above the arrows are the type III starting frequencies in MHz (from Benz *et al.*, 1983).

Klein *et al.* (1987) have also detected a preflash phase from their novel approach studying the onset phases of the hard X-ray emission rather than the times of the highest counting rates that are usually emphasized. They argue that the time of peak flux depends not only on the energization process but also on the dynamical evolution of the particles. The starting times, on the other hand, should be less affected by the particle transport and interaction processes. To investigate this possibility they have determined the start time of ten large flares detected with HXRBS as a function of the X-ray energy. An example of their results is shown in Figure 6. They find that two phases can be

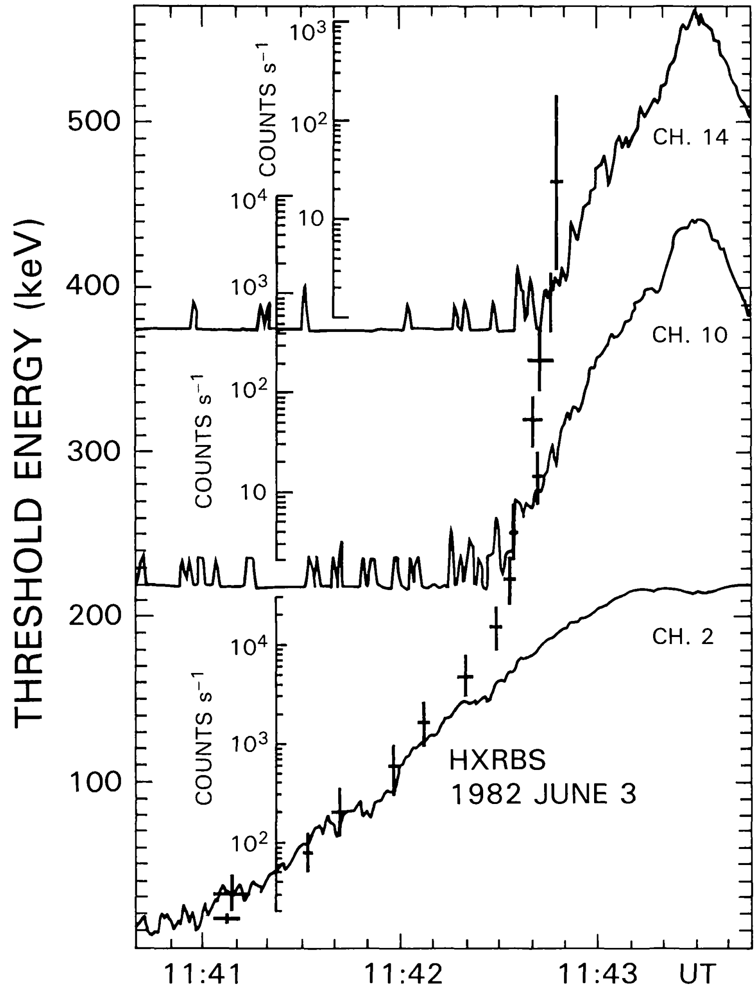

Fig. 6. Time history of the hard X-ray emission at the onset of the 3 June, 1982 flare. Crosses denote the photon energy where the count rate exceeds the noise level. The dashed curves give the count rate in three HXRBS detector channels on a logarithmic scale: Channel 2 (37–62 keV), Channel 10 (262–294 keV), and Channel 14 (400–438 keV) (from Klein *et al.*, 1987).

distinguished in the hard X-ray emission. In the first, preflash, phase the emission is detected up to an energy limit ranging from some tens of keV to 200 keV. In the second or flash phase the count rates in all detector channels up to the highest energies observed with HXRBS of ~ 500 keV rise simultaneously to within a few seconds. This is equivalent to the X-ray spectrum becoming harder at this time. In two events, emission at higher energies including the gamma-ray line region from 4–8 MeV was observed to begin close to this same time. Microwave emission at 8.4, 19.6, and 35 GHz also reflects a hardening of the electron spectrum in that the highest frequency emission becomes the most intense at the start of the flash phase.

3.2. Periodic or Quasi-Periodic Variations

Much effort has been expended in searching for periodic fluctuations of the hard X-ray emissions in solar flares but no convincing evidence of more than a few equally spaced peaks has ever been found. Parks and Winckler (1971) reported five successive maxima with a periodicity of 16 s. Lipa (1978) reported many peaks in the power spectra of many hard X-ray bursts observed on OSO-5. None were shown to have any physical significance or to represent precise periodicity for more than a few cycles except possibly for one event first reported by Frost (1973) and shown in Figure 7. This event on

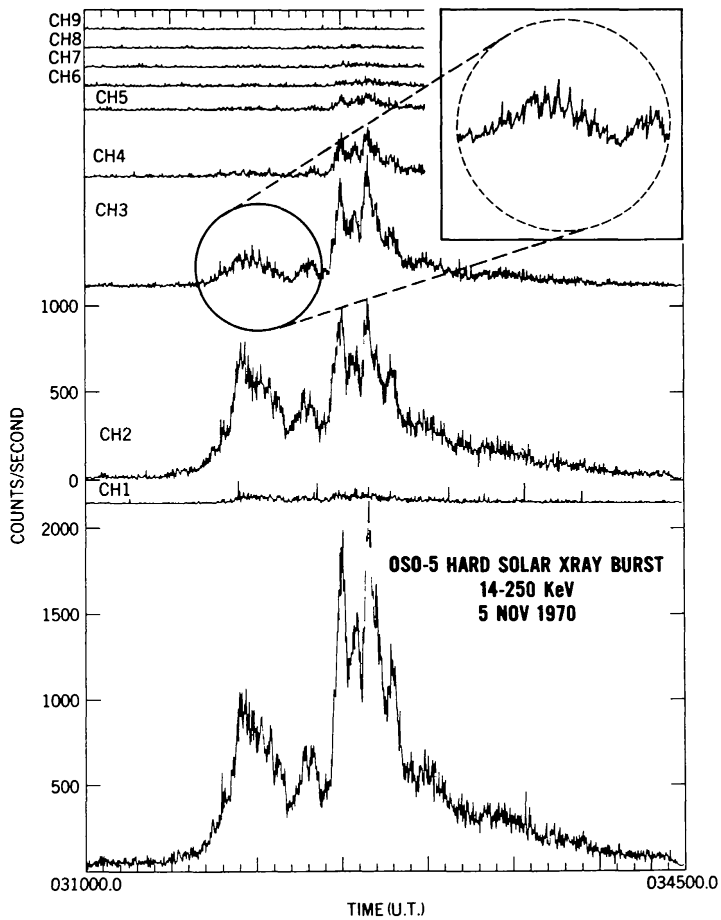

Fig. 7. Intensity-time profiles of X-ray burst observed on 5 November, 1970 showing the 7 min interval containing significant oscillations with a period of 26.9 s (from Frost, 1973).

5 November, 1970 was also recorded simultaneously at radio frequencies between 100 and 200 MHz by Wild (1973). Clear, periodic structure lasting for ~50 cycles was strikingly evident in the radio data with a period of 1.8 s. The hard X-ray observations obtained by sampling the flux every 2 s showed a peak at 26.9 s in the power spectrum for a seven minute interval some 15 min before the radio periodicity. This was interpreted by Frost as resulting from the beating between the 2 s and 1.8 s periodicities. The data were interpreted according to McLean *et al.*'s (1971) model in which the pulsation occur when a type II radio burst excites oscillations in a magnetic loop. The 15-min delay between the X-ray and radio periodicity was attributed to the shock travel time at a velocity calculated to be 580 km s^{-1}. Unfortunately, no similar observations have ever been reported where the X-ray time resolution would have been sufficient to resolve the fundamental component of the oscillations.

More recently, Kiplinger *et al.* (1982) and Kiplinger (private communication) have made a power spectrum search for periodic oscillations in 137 flares observed with HXRBS. They find that significant periodicities with frequencies between 0.05 and 50 Hz rarely, if ever, occur in the hard X-ray emission. The best case is the one shown in Figure 8, where two peaks that could be the fundamental and the first harmonic of

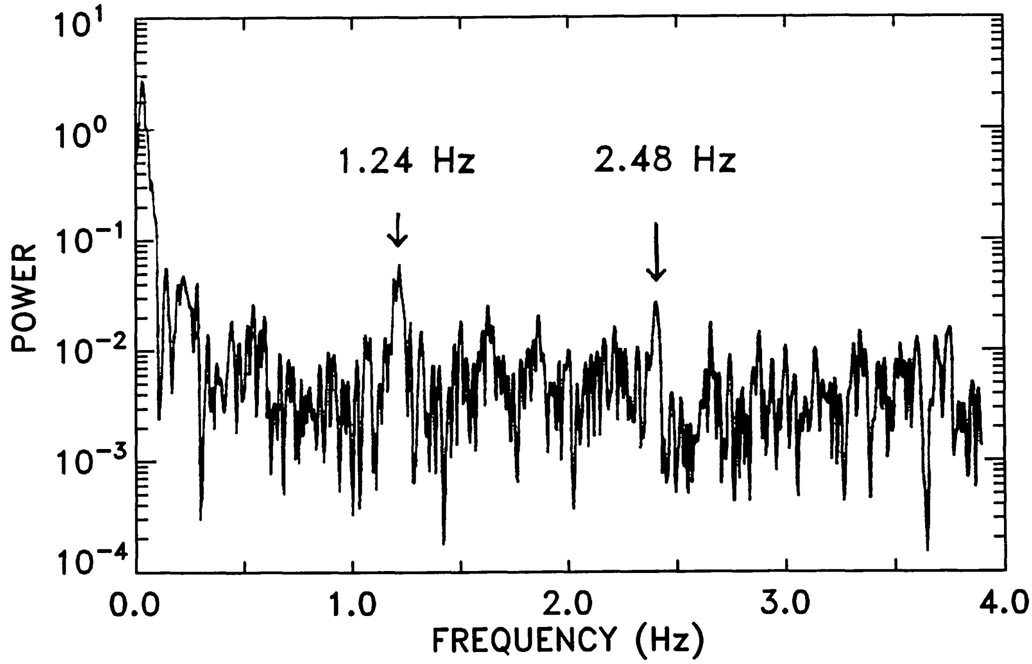

Fig. 8. Hard X-ray power spectrum of the flare of 12 July, 1980 that peaked at 17:36:15 UT (from Kiplinger *et al.*, 1982). Data for HXRBS Channels 1 and 2 only were used on the decay of the event from 17:36:20 to 17:37:25 UT. The combined chance probability of obtaining the observed peaks at 1.24 and 2.48 Hz is 1 in 18000, assuming that they are at the fundamental and first harmonic frequencies of a periodic variation in this time interval.

the pulsations are evident at 1.24 and 2.48 Hz in the power spectrum of the HXRBS counting rates in Channels 1 and 2 (i.e., 28–55 keV) during the decay of an event on 12 July, 1980. The combined probability from Poisson statistics of getting two peaks with the measured amplitudes that are separated by exactly a factor of two in frequency is one in 18000. The periodicity was, however, not found in the Berne 8.4 GHz data or in the HXRBS data at higher energies.

A somewhat different approach has been taken by Desai *et al.* (1987) in their search for periodic behavior of the hard X-ray emission. They argue that the basic pattern may not be sinusoidal but may consist of short spikes that would not be efficiently revealed in a power spectrum analysis. Consequently, they have carried out superposed epoch analysis on a number of likely events and present evidence for interwoven repeating patterns of bursts. They find several cases of flares showing two or more interlaced series of spikes with separations between spikes in the same series of 1 to 5 s but with a maximum of seven spikes in any one series. Their best example is shown in Figure 9.

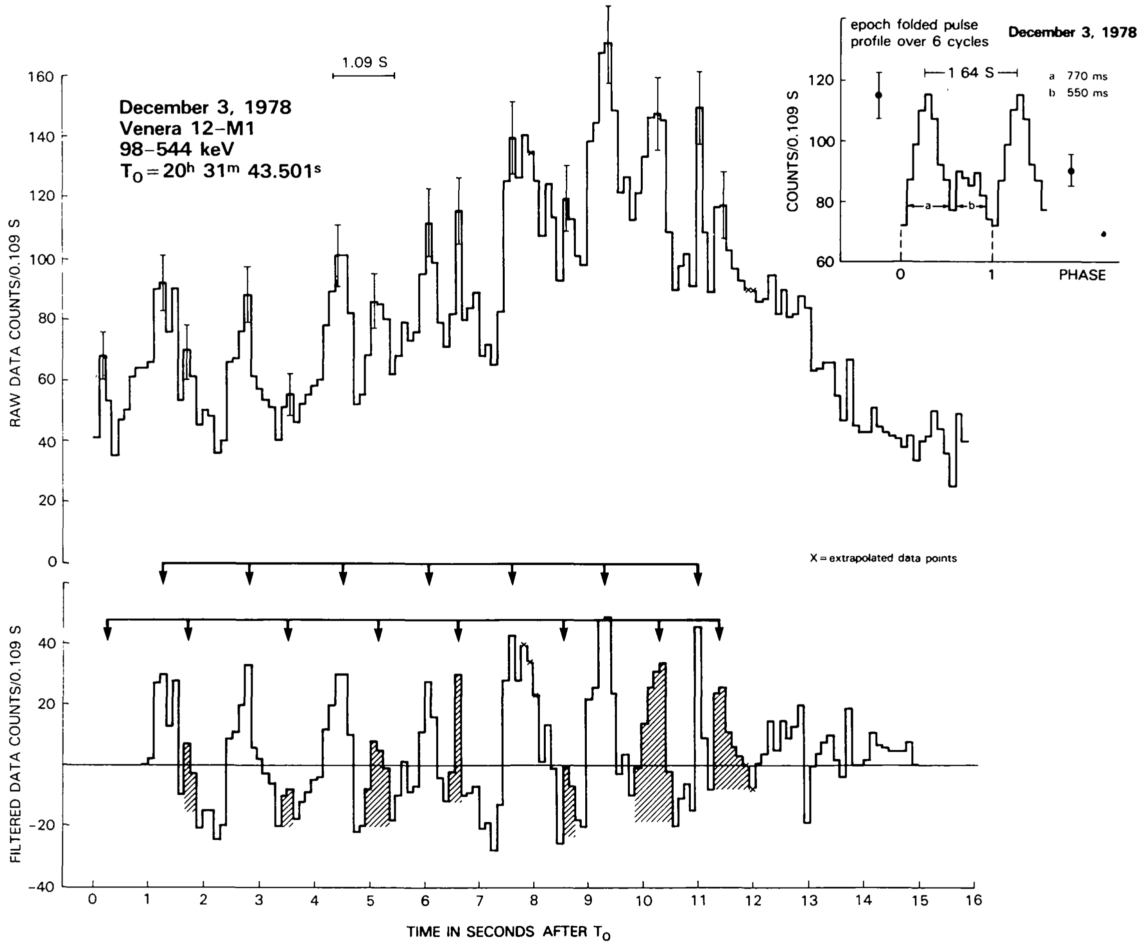

Fig. 9. Time history of the 3 December 1978 event (from Desai *et al.*, 1987). Arrows above the filtered time history shown below indicate the two synchronized time series.

They have interpreted these results on the basis of the model of Zaitsev and Stepanov (1982) and Zaitsev, Stepanov, and Chernov (1984), in which compact magnetic loops act as resonators for fast-mode MHD waves. While these results are interesting and suggest that individual loops can produce multiple periodic spikes, the evidence is circumstantial with little supporting data, and the analysis technique can become subjective.

In contrast to the evidence for strict periodicity, reports abound of quasi-periodicity but the question of whether individual peaks originate from the same or a different location remains generally unanswered. The most famous and best studied case of a flare showing quasi-periodic peaks is the event on 7 June, 1980 (Kiplinger *et al.*, 1983; Kane *et al.*, 1983; Forrest and Chupp, 1983; Nakajima *et al.*, 1983). Seven well separated peaks were detected in hard X-rays (shown in Figure 10), microwaves and γ-rays with separations ranging from 6.3 to 10.2 s. Kiplinger *et al.* (1983) present evidence in Figure 10 and 11 for three later distinct impulsive phases separated from each other by 75, 103, and 75 s with apparently similar time structures though with much reduced amplitudes.

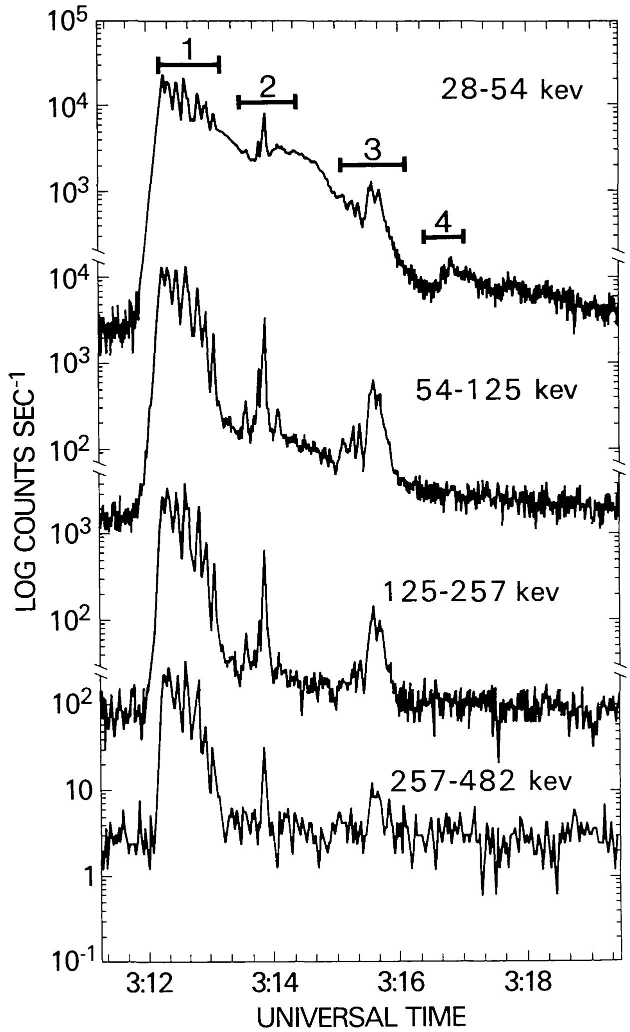

Fig. 10. Hard X-ray time profiles of the flare of 7 June 1980 in four energy ranges. Four impulsive phases are identified by the numbered horizontal bars above the uppermost curve (from Kiplinger *et al.*, 1983).

Various explanations of this remarkable event have been presented but any interpretation suffers from the lack of hard X-ray spatial information since HXIS was pointed at a different active region. Emslie (1981) has suggested that this event could result from seven adjacent loops firing in sequence. In his model the strong heating produced after the first loop flares results in a lateral expansion of the flux tube when the gas pressure exceeds the capability of the surrounding magnetic field to confine the high-pressure plasma. This lateral expansion may drive the field lines into a neighboring loop causing magnetic reconnection and another flare burst to occur. The repeated impulsive phases could be produced by reflaring of the same set of seven loops with the intensity of each occurrence being successively reduced because of the decrease in the stored magnetic energy. Kiplinger *et al.* (1983) even suggest the possibility that the seven loops fire in reverse order to explain the time profile of the third impulsive phase.

A different model has been proposed by Sakai *et al.* (1987) to explain the 7 June, 1980 event. In their model, the energy release is the result of the nonlinear coalescence

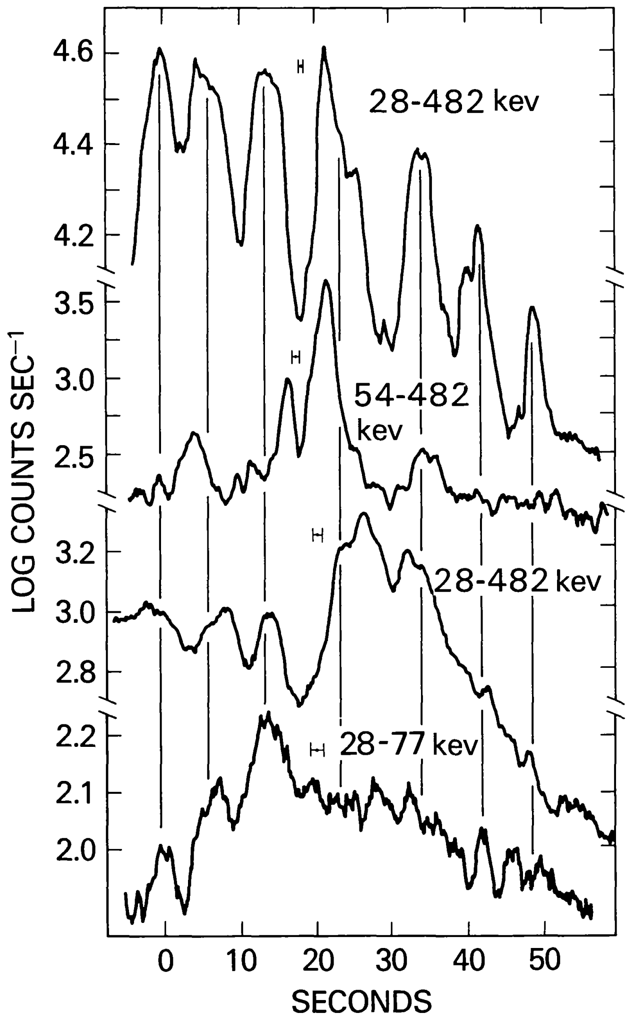

Fig. 11. The four impulsive phases of the flare of 7 June, 1980 arbitrarily shifted in time to align features. Energy ranges have been selected to enhance impulsive features (from Kiplinger *et al.*, 1983).

instability of current carrying magnetic loops (Tajima *et al.*, 1982). The double sub-peak structure, seen most clearly in the 17 GHz time history plots for some of the seven major peaks, is a characteristic predicted by this model as shown in Figure 12. The model is based on the fact that two parallel current loops are unstable against the coalescence instability. The two loops are attracted by and collide with each other and finally coalesce explosively into one loop with the release of a large amount of poloidal magnetic energy. Such a model can explain the simultaneous acceleration of electrons and ions observed in this and other flares (Forrest and Chupp, 1983) and also the multiple quasi-periodic peaks. The time between peaks is about one Alfvén transit time. Such a model can also be applied to more gradual flares such as the event on 26 November, 1982. In this case the loops are believed to coalesce more slowly but the magnetic reconnection of the poloidal magnetic field is still more rapid than in the classical tearing mode. The model again explains the three structures in this event each with characteristic double sub-peaks.

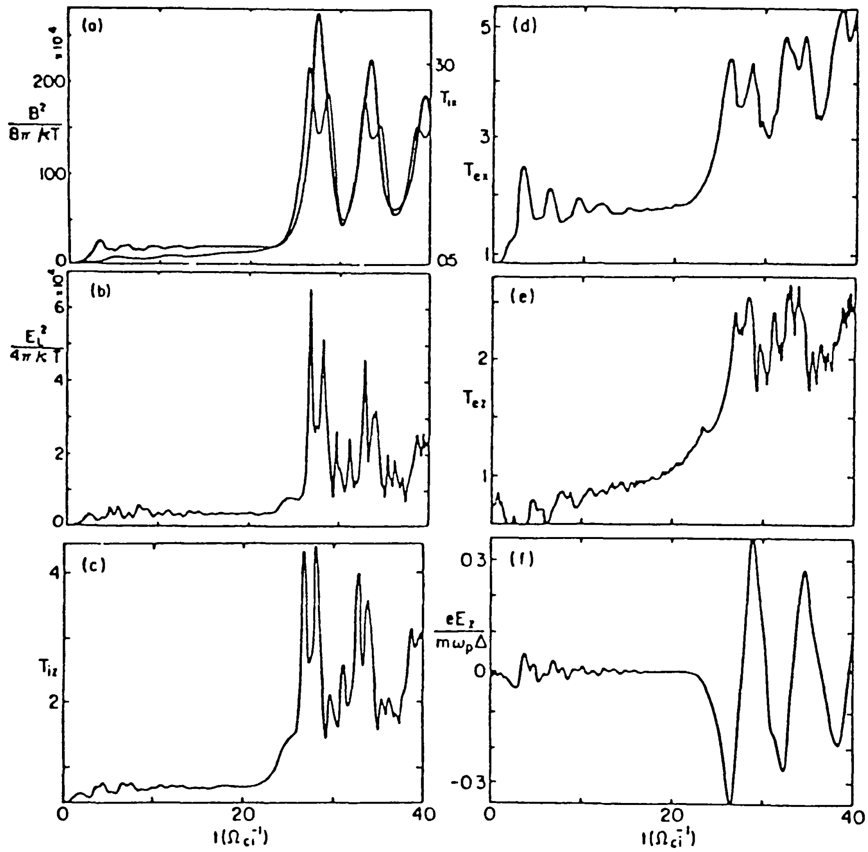

Fig. 12. Temporal profiles of particle and field quantities for the coalescence process (from Sakai *et al.*, 1987). (a) The thick line represents the magnetic energy, the thin one the ion temperature in the X-direction. (b) Electrostatic field energy. (c) Ion temperature in the Z-direction. (d) Electron temperature in the X-direction. (e) Electron temperature in the Z-direction. (f) Inductive electric field (E_z).

4. Spatial Observations

The spatial information concerning hard X-ray emission from solar flares has been obtained by four basic methods:

(i) Direct imaging at energies below ~30 keV.

(ii) Stereoscopic observations using two widely separated detectors at energies ≥100 keV.

(iii) Observations of events that are partially occulted by the solar limb or by the Moon.

(iv) Variations as a function of heliocentric longitude (limb darkening or limb brightening).

Methods (ii) and (iii) have sometimes been combined together for specific flares.

The single word that can be used to describe all of these techniques to date is 'inadequate'. The results are inadequate to answer any of the fundamental questions concerning energy release and particle acceleration, particularly during impulsive flares. The great potential of hard X-ray spatial information remains, however, and improvements by an order of magnitude in the spatial resolution to ≤1 arc sec and in the time resolution to < 1 s will allow new observations to resolve the more fundamental distance and time-scales of a typical flare.

In spite of this considerable gap between the observations that are currently available and those that will be ultimately required, much progress has been made over the last decade.

4.1. Direct Imaging

Results from the two imaging spectrometers, the Hard X-Ray Imaging Spectrometer (HXIS) on NASA's SMM, and the Solar X-Ray Telescope (SXT) on the Japanese Hinotori have been instrumental in establishing three different forms of flare – types A, B, and C as discussed earlier. Imaging observations are discussed here briefly, but only for type B events. The reader is referred to previous reviews by Tsuneta (1983), Dennis (1985), de Jager and Švestka (1985), and Tanaka (1987) for more detailed discussions.

4.1.1. *Type B Flares*

The review by Dennis (1985) of the SMM observations of one well observed flare on 5 November, 1980 shows the extent of the debate over the images of type B flares. Basically, the images of this flare show two bright patches of hard (16–30 keV) X-ray emission separated by ~30″ at the time of the impulsive peak of the event. A third patch some 70″ away also brightens simultaneously (to within the ~10 s effective time resolution of the observations). Initially, these images and results for similar events observed on 21 May and 10 April, 1980 were presented as strong evidence for the existence of electron beams (Hoyng *et al.*, 1981; Duijveman, Hoyng, and Machado, 1982). The electrons were envisioned as propagating from the acceleration site near the top of a coronal magnetic loop or loops down the legs to the footpoints, where they lost their energy to the ambient electrons by Coulomb collisions and coincidentally produced the observed bremsstrahlung X-rays in interactions with the ambient ions.

The HXIS data for the 5 November, 1980 flare has been analyzed using several different techniques:

Hoyng *et al.* (1981) treated the raw data with no image deconvolution.

Dennis *et al.* (1986) used the deconvolution method given by Švestka *et al.* (1983).

MacKinnon (1983) and MacKinnon, Brown, and Hayward (1985) used a maximum entropy routine to produce deconvolved images.

Machado, Rovira, and Sneibrun (1985) made assumptions about the X-ray source and convolved the predicted distribution through the instrument response function. A single loop of constant cross-section was assumed with the electron acceleration at the loop top.

From these several different analyses one is forced to conclude that separate bright patches of hard X-ray emission do occur from the ends of magnetic loops but their existence does not necessarily imply preferential emission from the loop footpoints as expected in a thick-target model. Machado, Rovira, and Sneibrun (1985) state that 'the data are not inconsistent with large acceleration efficiencies of >20%', while MacKinnon, Brown, and Hayward (1985) "... do not consider the HXIS 'footpoint' data as supporting a conventional thick-target beam interpretation...".

One important result obtained by MacKinnon *et al.* is that the 16–30 keV footpoint X-ray fluxes obtained from the HXIS data are only 15–28% of the flux extrapolated from the HXRBS spectra at higher energies. Taken at face value, this implies that not all of the HXRBS emission comes from the HXIS footpoints. The possibility that the spectrum may flatten at energies below 30 keV could explain this result but the HXIS data suggest that the footpoint are in fact much softer than the HXRBS spectrum. Uncertainties in the instrument calibrations could explain the difference in the extrapolated flux levels but it is more difficult to understand the difference in the spectral index between the two instruments.

MacKinnon, Brown, and Hayward (1985) have shown that in view of the poor statistics, the poor time resolution of the observations, and the $8'' \times 8''$ image pixel size, it is impossible to differentiate between an electron beam and a thermal model interpretation of the observations. While the images are consistent with X-rays from the footpoints of loops expected in the beam model, they are also consistent with a loop filled with plasma at $> 10^8$ K. In the latter, thermal, case the two bright patches result from the greater thickness of plasma seen in the legs of the loop over the footpoints compared to the thickness seen through the top of the loop. The two factors which could most clearly differentiate between the two models, namely the simultaneity of the footpoint brightenings and the contrast between the bright patches and the intervening area, were not measured with sufficient accuracy to reject either model. The most widely separated bright patches were observed to brighten simultaneously to within the ~ 10 s HXIS time resolution but an electron beam could traverse the loop in ~ 1 s and a thermal conduction front in ~ 10 s. The greatest contrast between footpoint and loop-top brightness required by the observations of any flare is ~ 3 to 1. MacKinnon, Brown, and Hayward (1985) estimate that you might expect to see a contrast as high as 5 to 1 for a loop filled with thermal plasma while the electron beam model would give much higher values at 20 keV provided the density in the loop was low enough so that a 20–30 keV electron could reach the footpoints without losing a significant fraction of its energy, i.e., $\leq 10^{10}$ cm^{-3} for a loop $30''$ long.

One of the major objectives of future observations must be to follow the evolution of the X-ray spectrum as an electron beam or a thermal source propagate along a loop with a typical length of $10''$ and cross-sectional diameter of $1''$. The evolution of such a loop as it would appear in hard X-rays for the two models is shown schematically in Figure 13 together with the temporal and spatial resolution of HXIS and of a possible future imager. The observations must have sub-second time resolution to resolve the time-scales of typical variability observed in the impulsive phase and the images must be such that a contrast of > 10 between a bright source and a neighboring weaker source can be accurately measured. Important length and time-scales for future observations are given by the time and distance that a 30 keV electron will travel while producing the bulk of its hard X-ray emission. In a medium with a density of 3×10^{11} cm^{-3}, typical of a dense flare plasma, the time is ~ 20 ms and the distance is ~ 2000 km or 3 arc sec. The electron spectrum would be expected to change substantially on these time and distance scales and the way in which it changes could be expected to be very different for beam and thermal models.

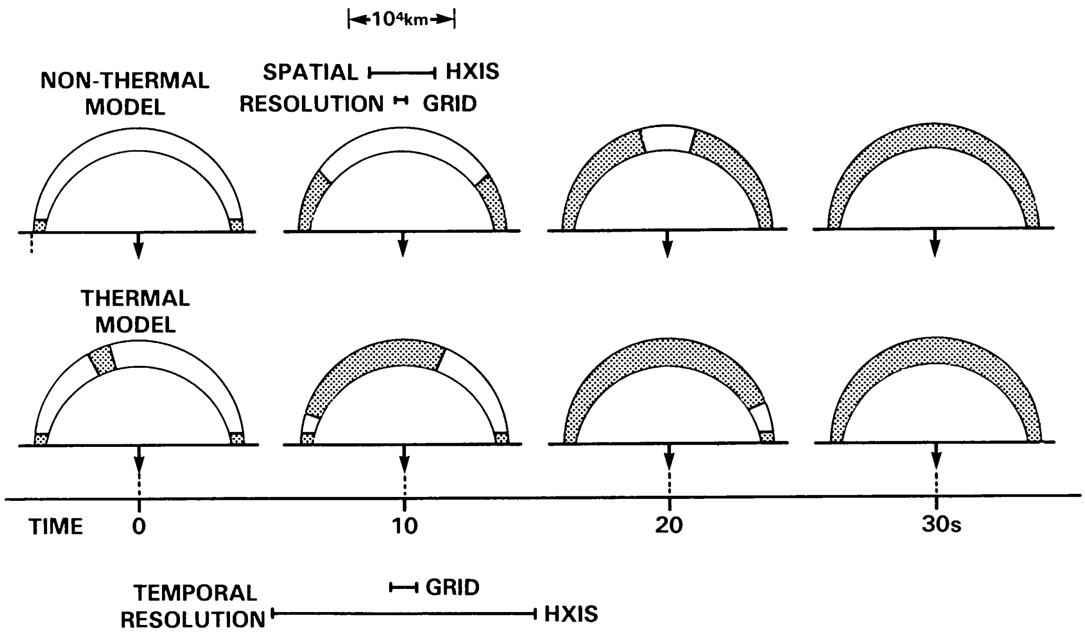

Fig. 13. The evolution of a typical flaring magnetic loop as it would appear in 20 keV X-rays for the thermal and nonthermal models. The top and bottom row of loops show the expected evolution of the hard X-ray spatial structure in the nonthermal and thermal models, respectively. Shown above and below the figure are the spatial and temporal resolutions of HXIS and GRID, a proposed imager using the Fourier-transform technique to achieve arcsecond spatial resolution.

4.1.2. *Type C Flares*

The situation is somewhat less uncertain than for type B flares with respect to the interpretation of the images of type C flares although fewer of these have been observed. The canonical type C flare on 13 May, 1981 was reported by Tsuneta *et al.* (1984). The hard X-ray source is clearly offset by ~ 1 arc min towards the limb from the two-ribbon Hα flare indicating an altitude of ~4 × 10^4 km. This is in agreement with the altitude of the microwave source derived from one-dimensional imaging at 35 GHz (Kawabata, Ogawa, and Suzuki, 1983).

The main questions concerning this type of source that future imaging observations must answer is how does the X-ray spectrum evolve in time and space and what is the altitude distribution of the source. This information is required to separate the effects of energy losses and continued acceleration, both of which can contribute to the spectral hardening seen throughout these events.

In one sense, observations of this type of flare are easier than those of the impulsive type B flares since the time and distance scales are significantly greater being tens of seconds and tens of arc sec, respectively. However, the source can be quite large extending to 70″ × 30″ for the 30 May, 1981 flare, and it then becomes a challenge for some types of imagers, such as those using the Fourier-transform subcollimator technique (Hurford and Hudson, 1980; Crannell *et al.*, 1986; Prince *et al.*, 1988), to image such an extended source. The VLA also has difficulty since it uses the same mathematical principle for obtaining images. Mellozzi, Kundu, and Dennis (1988) observed a type C flare on 14 November, 1981 with the VLA in the 'C' configuration and found that only $\sim 10\%$ of the flux was imaged at 6 cm and $\sim 20\%$ at 20 cm during the peak of the event. They concluded that the source must have been greater than ~ 100 arc sec in extent and was probably at an altitude of $4-5 \times 10^4$ km.

4.2. Stereoscopic observations

Brown and McClymont (1975) noted that the most promising method of distinguishing between thick- and thin-target models of hard X-ray flares was from the distribution of the source height with altitude in the solar atmosphere.

Unique information on the altitude of hard X-ray sources above ~ 100 keV has been obtained from five flares observed stereoscopically with the spectrometers of the International Sun Earth Explorer-3 (ISEE-3, now renamed the International Cometary Explorer, ICE) and the Pioneer Venus Orbiter (PVO) spacecraft (Kane, 1983). By concentrating on flares that were partially occulted over the limb as seen from one spacecraft but fully observed by the other, a measure of the altitude distribution of the photon source and its dependence on the photon energy and time during a flare can be determined. Basically, Kane found that for impulsive flares about 95% of the ~ 150 keV X-ray emission originates at altitudes of $\lesssim 2500$ km.

Brown *et al.* (1983) and MacKinnon (1986) conclude that for the three events with the occulting altitude ranging from 0 to 2500 km the results are consistent with the thick-target model but for the two events with the occulting altitude $> 25\,000$ km the results are inconsistent with this model. Kane (1983) concluded that for impulsive flares, "... the thick-target and the dissipative thermal model are partially in agreement with the observations ..." but that the thermal model with adiabatic compression of a magnetically-confined plasma and the thin-target model are not consistent with the observations.

For gradual flares, the effective height of the sources reported by Kane (1983) was greater than that of the impulsive bursts but $\gtrsim 70\%$ of the 100–500 keV emission was found to come from altitudes of $\lesssim 2500$ km. Thus, the observations are not consistent with a purely coronal source but they are consistent with a model that has both trapped and precipitating electrons.

5. Spectral Measurements

5.1. Spectral evolution

It is clear that the hard X-ray spectrum is, in general, relatively soft at the start of the impulsive phase, becomes hardest at the peak of the event, and softens as the rate decreases. This general soft-hard-soft signature, typical of type B flares, was recognized by Kane and Anderson (1970) and has been confirmed more recently by many workers (e.g., Dennis, Frost, and Orwig, 1981; Dennis, 1985). It is, however, only part of the picture. Hoyng, Brown, and van Beek (1976) showed that in some events the spectrum continues to harden even as the emission decreases in intensity. We now know that this soft-hard-harder spectral behavior is characteristic of the so-called gradual or type C flares (Tsuneta, 1983; Dennis, 1985; Cliver *et al.*, 1986a, b).

Even in an impulsive event, Lin *et al.* (1981) and Lin and Schwartz (1987) have shown more complex spectral behavior than the simple soft-hard-soft signature. They used high-purity germanium (HPGe) detectors cooled with liquid nitrogen to obtain much higher energy resolution than is possible using any scintillation detector such as NaI(Tl), CsI(Tl), or CsI(Na). The FWHM resolution of their HPGe detectors was <1 keV between 15 and 200 keV compared to the 10 to 50 keV typical at 60 keV for scintillation detectors. With such super-high resolution and the good fortune to detect a substantial

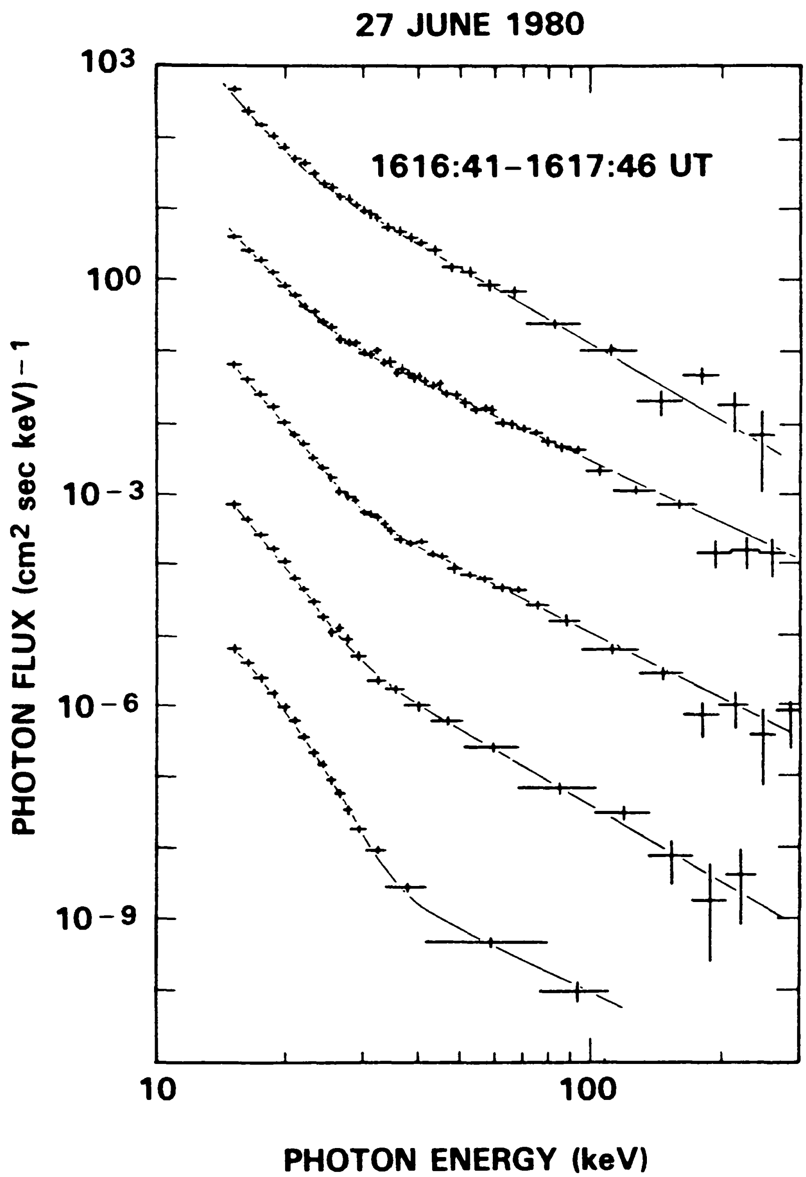

Fig. 14. High-resolution hard X-ray energy spectra for a solar flare on 27 June, 1980 obtained with an array of cooled high-purity germanium detectors flown on a high-altitude balloon. The vertical scale applies to the uppermost spectrum, with each succeeding spectrum offset downward by two decades. The component of the hard X-ray spectrum from a superhot plasma at 34×10^6 K is clearly seen below about 30 keV and becomes more dominant with time over the power-law component seen at high energies (from Lin *et al.*, 1981).

flare in an observation that lasted only 141 min on a balloon flight on 27 June, 1980, they were able to track the spectrum in detail above 13 keV throughout the event on time-scales as short as 1 s or less.

The major findings from this observation are as follows:

(1) At energies below ~35 keV, an extremely steep X-ray spectrum characteristic of an isothermal plasma appeared at the peak of the impulsive burst and became increasingly dominant as the flare progressed (Lin *et al.*, 1981; Lin, Lin, and Kane, 1985). Successive spectra showing the appearance of this component are shown in Figure 14. They reveal, for the first time, a super-hot component of a flare with a temperature that reached as high as 34×10^6 K, much higher than the $< 20 \times 10^6$ K typically measured in the soft X-ray spectral range. Furthermore, this thermal spectrum was extremely steep in the 13 to 30 keV range being equivalent to an E^{-11} spectrum if fitted with a power

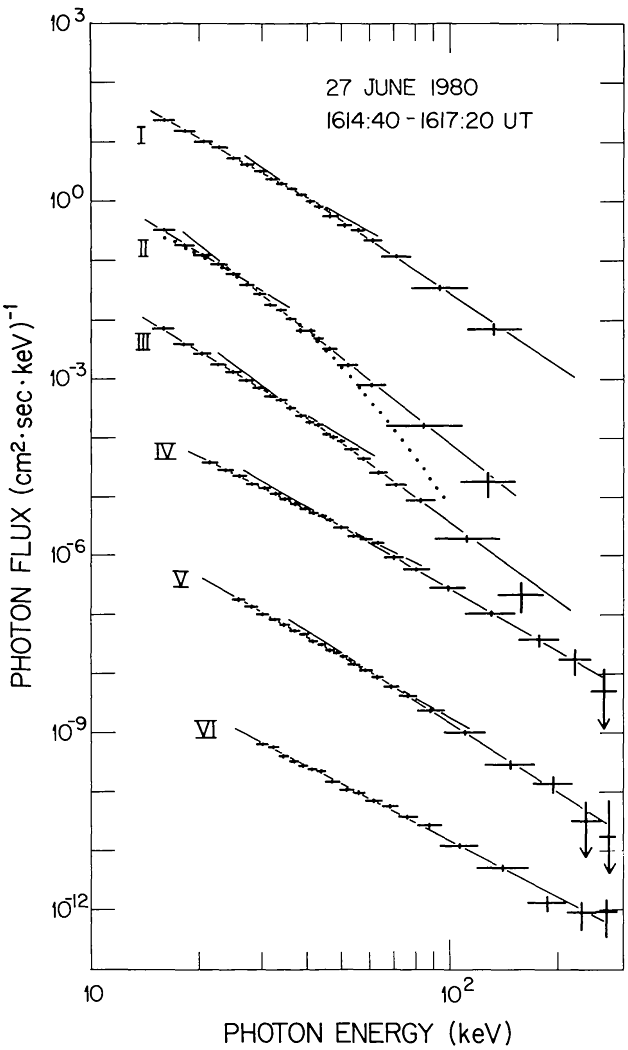

Fig. 15. High-resolution hard X-ray energy spectra similar to those shown in Figure 14 showing the high-energy component for six intervals during the same flare. The vertical scale applies to the uppermost spectrum, with each succeeding spectrum offset downward by two decades. The best double power-law model fits (single power-law for spectrum VI) are shown by the solid lines. For comparison the best isothermal model fit (dotted curve) is shown for spectrum II (from Lin and Schwartz, 1987).

law (where E is the proton energy). No scintillation spectrometer can resolve such a steep spectrum. Thus, all previous hard X-ray spectral measurements below ~50 keV are subject to misinterpretation, particularly later in the impulsive phase. More importantly, this super-hot component may contain significant flare energy (10^{28}–10^{31} ergs in the flare observed) and, because its conduction and radiation times are so short, it can reveal details of the short-term rate of energy release in the flare.

(2) Prior to the appearance of the super-hot component, the high resolution spectral observations show conclusively that the spectrum is not consistent with a single power law or with an isothermal spectrum. Successive spectra recorded during the early part of the flare are shown in Figure 15. The simplest spectral form consistent with the data is a double power law that is steeper at higher energies. Two superimposed components of the double power-law spectrum were identified from the time variations: impulsive spikes lasting 3–15 s with a break energy of 30–65 keV and a more slowly varying, softer component with a break energy that increased from 25 keV to > 100 keV as the flare progressed. Lin and Schwartz (1987) argue by analogy with the situation in the Earth's auroral zone that this double power-law shape indicates that the electrons were accelerated in a DC electric field. This would produce an electron spectrum of the form shown in Figure 16 and this in turn would result in the observed double power-law

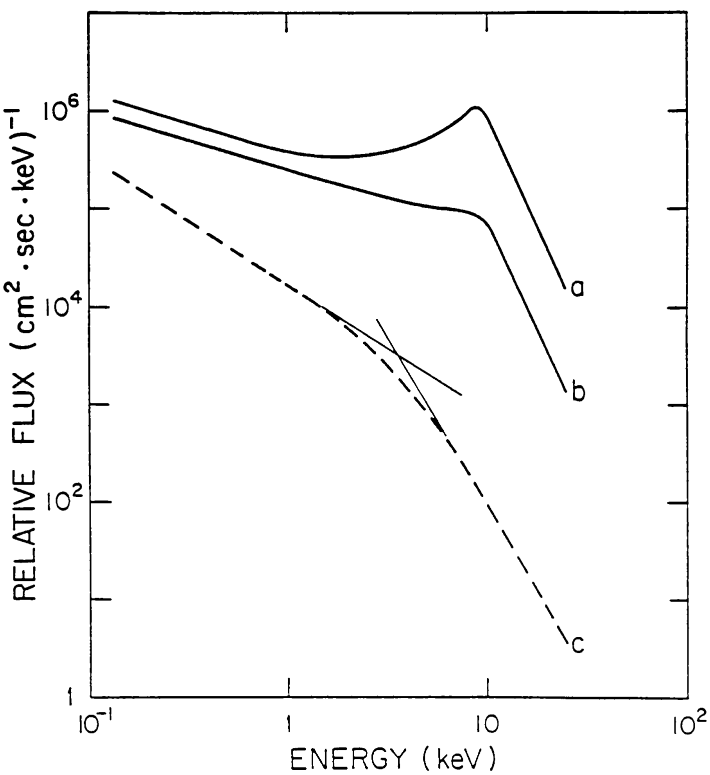

Fig. 16. Electron spectra in the Earth's auroral zone. Curve (a) is a typical electron spectrum observed at a single point, showing the peak corresponding to the DC potential drop. Curve (b) shows the spectrum integrated across an auroral arc. Curve (c) gives the bremsstrahlung X-ray spectrum that would be produced in thick-target interactions by electrons with a spectrum shaped as in curve (b) (from Lin and Swhartz, 1987).

spectrum. If this model can be verified, it is clearly of great importance for any flare model and shows the great potential for future high-resolution hard X-ray spectral measurements.

Even though these results were obtained for just one flare, they demonstrate that there is much useful information to be obtained from high-resolution measurements of the hard X-ray spectrum. It is not merely a continuum with a rather uninteresting and not very informative power-law or exponential shape as has frequently been assumed.

5.2. Total energy in electrons

One of the valuable flare parameters that can be estimated from the hard X-ray spectral measurements is the total energy in electrons. The value obtained depends significantly on the model assumed for the hard X-ray source, whether it is thick-target, thermal, or some combination such as a thin-target trap plus precipitation into a thick target. Nevertheless, it is instructive to compute the energy in fast electrons required by the hard X-ray observations and compare the values obtained with other estimates of flare energies, particularly the maximum energy in the thermal plasma that emits the soft X-rays. The techniques to compute the total energy in fast electrons according to a

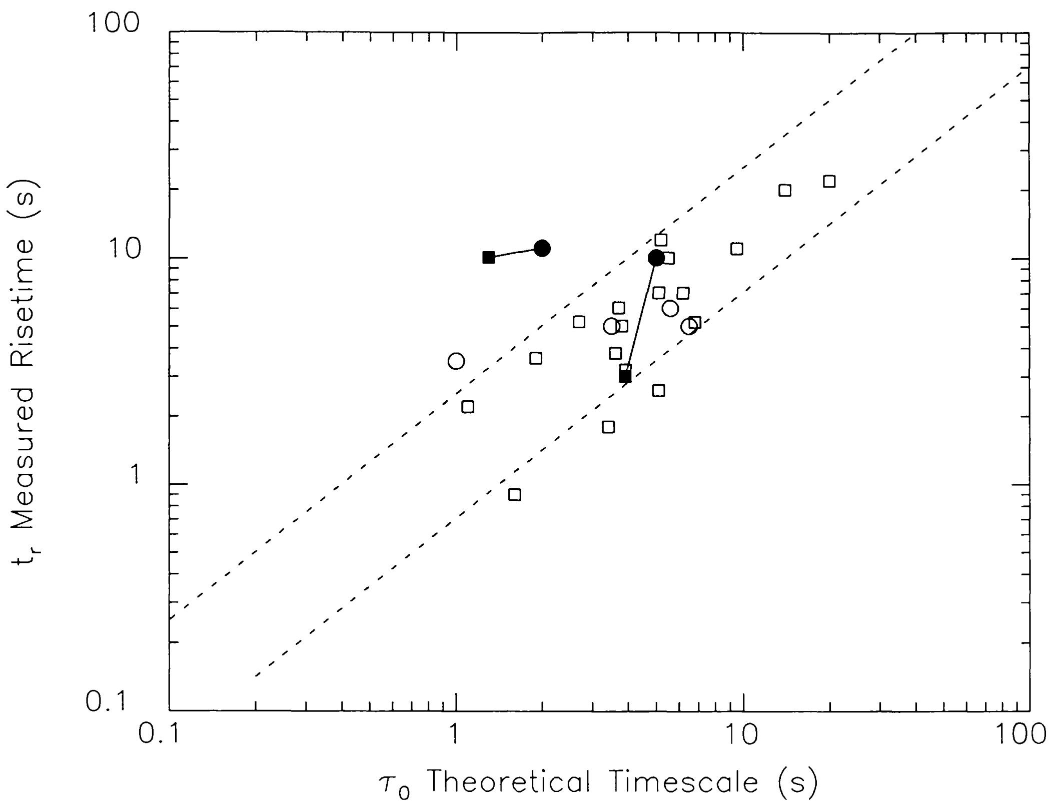

Fig. 17. Plot of the log of the measured rise time of the hard X-ray burst versus the log of the theoretical rise time for 20 events (squares) from Batchelor *et al.* (1985) and the six events from Starr *et al.* (1988) (circles). The dashed lines are boundaries of the expected positions of disk points, if the sources are arches from 2 to 4 times as long as they are wide. The two pairs of connected points designate events the two data sets have in common (from Starr *et al.*, 1988).

thick-target and a thermal model are presented by Wu *et al.* (1986). They present computed values of the energy in electrons above 25 keV for 30 flares observed with HXRBS and HXIS in 1980.

Note that a lower energy cut-off must be imposed on the power-law electron spectrum used by Wu *et al.* to ensure that the total energy computed as the integral of this power law stays finite. The appropriate value of this cut-off energy is unknown but the values obtained for the total energy in the electrons varies by orders of magnitude depending on the value chosen. There is no convincing evidence for a flattening at lower energies in the observed X-ray spectrum as would be expected if there was a lower energy cut-off or flattening in the electron spectrum. The problem of searching for such a flattening is exacerbated by the increasing thermal component at lower energies during the impulsive phase. This thermal component varies more gradually, however, so that, in principle, taking the spectrum of just the impulsive component should at least reduce the problem. Kiplinger (1987) reports an attempt to make an estimate of only the impulsive component for an intense spike observed with HXRBS and HXIS on 29 March, 1980. Even for this largest single spike yet reported (Dennis *et al.*, 1981), the statistics were too poor to reach any definite conclusions about the cut-off energy. The data were consistent with it being as high as 50 keV and the impulsive spike was not evident in the time profiles at energies below ~ 10 keV. Other groups have reported impulsive emission down to lower energies (Kahler and Kreplin, 1971; Peterson *et al.*, 1973; de Jager and Boelee, 1984; de Jager *et al.*, 1984) but it is not clear if the electron spectrum extends down to these energies since bremsstrahlung photons are produced at all energies below that of the source electron.

A more comprehensive approach has been attempted by Gabriel *et al.* (1984), who used observations from three of the SMM instruments covering photon energies from 4 to 500 keV including the high-resolution line spectroscopy of the Bent Crystal Spectrometer (BCS). They determined how consistent the observations of BCS, HXIS, and HXRBS were with various assumed differential emission measure (DEM) distributions plus power-law spectra at higher energies. For the flare on 29 June, 1980 at 18:23 UT, they find that the combined observations are not consistent with a purely thermal DEM distribution during the early stages of the impulsive phase. An additional power-law contribution is required to fit the data. Changing the cut-off energy of this power-law component from 10 to 15 keV had only a minor effect on the fitting. While this novel approach has not produced any surprises, it has the greatest potential for using the extensive data sets from different instruments covering the broadest possible energy range and should be applied to more events in the future.

Comparison of the total energy in electrons above 25 keV with the total energy in the thermal plasma that produces the soft X-ray emission by Wu *et al.* (1986) shows that there is a general correlation for the 19 flares presented. However, reducing the electron energy threshold below 25 keV would result in an embarrassingly large energy in fast electrons compared to the energy in the thermal plasma. Already, with a 25 keV threshold, all but four of the 19 flares considered by Wu *et al.* have more energy in fast electrons than in the thermal plasma. Note also that the energy in the thermal plasma has been computed assuming a unity filling factor for the soft X-ray emission imaged with HXIS. The energy of the thermal plasma depends on the square root of the filling factor, and values as small as 10^{-2} to 10^{-4} have been estimated for some flares (de Jager *et al.*, 1983; Wolfson *et al.*, 1983; Martens, 1985). Such small filling factors would destroy any similarity with the energy in fast electrons. Difficulties with the apparent large energy in fast electrons have lead Tanaka (1987) to suggest cut-off energies even higher than 25 keV for some flares.

5.3. Wide spectral range measurements

Further new information has recently been gained from the hard X-ray spectrum by measuring it over a wider energy range than has previously been possible. Yoshimori, Watanabe, and Nitta (1985a, b) have presented combined spectra for four flares measured with the hard X-ray and the gamma-ray spectrometers on the Japanese Hinotori spacecraft. The spectra extending from 20 keV to 7 MeV show variations from flare to flare but they all show significant hardening at energies above ~400 keV. All the flares were Hα 2B or greater and GOES X1 or greater. The power-law spectral index was between −3.2 and −4.0 at energies below 300 keV and all the spectra showed significant excess above an extrapolation of such a power law to higher energies.

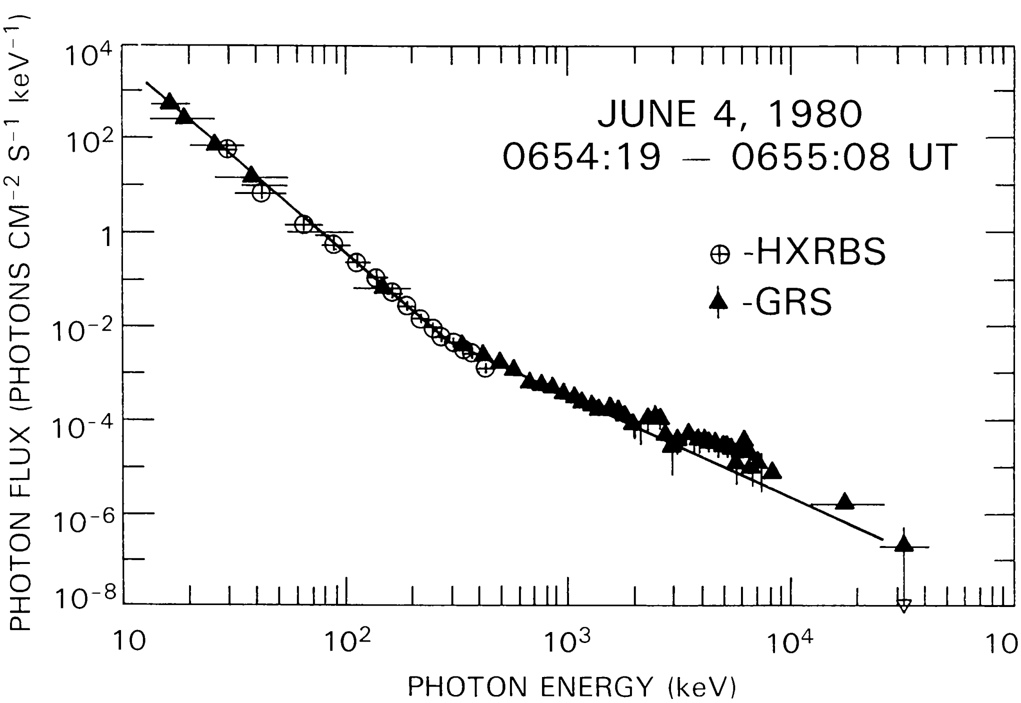

Fig. 18. Combined HXRBS and GRS spectrum for an event on 4 June, 1980 (Orwig and Forrest, private communication). Data points from the small hard X-ray detectors associated with GRS are also shown at energies below 200 keV. The horizontal line through each point represents the electronic channel width and the vertical line represents $\pm 1\sigma$ statistical uncertainties. The continuous line from 20 keV to 20 MeV represents a double power-law function fitted to the data points below 1 MeV. Note the break in the spectrum at ~300 keV with the power-law spectral index of −4.3 at energies below the break and −2.2 at higher energies. The contribution of the line emission above 1 MeV would tend to flatten the spectrum below 1 MeV but calculations show that even with this removed the power-law index would still be ≃ −2.5 above 300 keV.

Figure 18 shows a spectrum extending from a ~25 keV to 25 MeV obtained by combining the measurements of HXRBS and the Gamma Ray Spectrometer (GRS) on SMM for an event on 4 June, 1980. This combined spectrum also clearly shows hardening at energies above ~300 keV. The spectrum flattens from $E^{-4.3}$ below 300 keV to $E^{-2.2}$ from 300 keV to 1 MeV. In this case, it can be shown that the hardening persists even after the contribution to the Compton continuum below 1 MeV from the gamma-ray lines is removed. Similar hardening at high energies has been observed for other large flares seen with SMM but values of $\Delta\gamma$ (the difference between the spectral index at low and high energies) between 0 and ~2 have been obtained for different events (Orwig and Forrest, private communication).

Various possible explanations for the spectral hardening have been suggested including possible instrumental effects. The agreement between the SMM and Hinotori results and the variations between flares would seem to rule out any error resulting from the use of incorrect instrument response functions or other instrumental effects. More likely explanations relate to different physical proceses that result in the observed spectra. These include

(1) The effect of the gamma-ray lines on the continuum spectrum (this seems to have been ruled out, at least for the event shown in Figure 18).

(2) The increasing contribution of electron-electron bremsstrahlung and the higher bremsstrahlung efficiency of relativistic vs non-relativistic electrons. This should give a spectral hardening above ~500 keV but with $\Delta\gamma \sim 0.5$ (Vestrand, private communication) and so could not explain all of the hardening shown in Figure 18. Furthermore, it should be dependent only on the hardness of the spectrum and consequently should not differ substantially from flare to flare.

A likely explanation of the spectral hardening is that it reflects directly the spectrum of the bremsstrahlung producing electrons. In other words, the spectrum of the electrons accelerated in the flare cannot be a single power law but must include a high-energy excess. Such an explanation has been considered by Suri *et al.* (1975) and by Yoshimori, Watanabe, and Nitta (1985a, b) and would have to be included in any model of particle acceleration.

In a more radical model that reproduces the break in the spectrum at ~400 keV (see Figure 19), Heristchi (1986) has proposed that the X-rays are produced as inverse bremsstrahlung when high-energy protons interact with ambient electrons. This process, first discussed by Boldt and Serlemitsos (1969), has previously been rejected because of the large number of protons required to produce the observed flux of hard X-rays (Emslie and Brown, 1985). Such large numbers of protons above 10 MeV would produce 10^3 to 10^4 more nuclear gamma rays than observed. However, Heristchi claims that several different factors were overlooked or incorrectly computed in the previous analysis and that this model can in fact give the observed numbers of nuclear gamma-rays to within an order of magnitude. A possibly more serious problem with this model is the large numbers of pions that would be produced in nuclear interactions of the high-energy protons required to produce the observed gamma-ray continuum spectrum above 10 MeV. The electron/positron and gamma-ray decay products of these pions

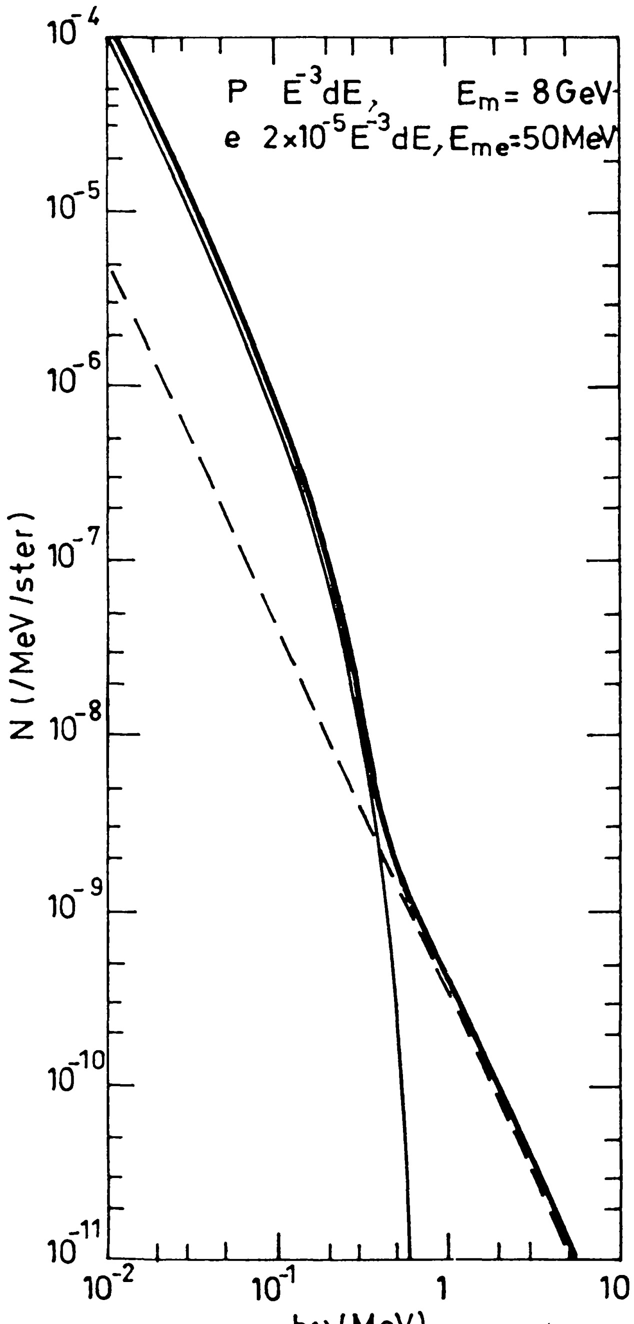

Fig. 19. Predicted X-ray spectrum from protons with a power-law spectrum for a flare at a heliocentric angle of 15° (from Heristchi, 1986). The dashed curve shows the X-ray spectrum from knock-on electrons and the solid line that falls steeply above ~500 keV represents the spectrum of inverse bremsstrahlung X-rays from the protons.

should result in far more gamma-rays in the 10–100 MeV range than are observed with GRS (Forrest, private communication). Thus, while this model is intriguing, it seems to be beset with at least two problems that make it inconsistent with the gamma-ray observations.

Simnett (1986) has summarized the arguments in favor of a dominant energetic role for low-energy protons. Unfortunately, the only observation that has been suggested to definitively determine the flux of protons below ~ 1 MeV is to search for a red-shifted component of the Lα line at 1215 Å (Orrall and Zirker, 1976). Such a component could be expected if a significant flux of downward-directed protons are produced during a flare. Some of the protons pick up electrons in charge-exchange interactions with the ambient atoms to produce hydrogen atoms in excited states moving with approximately the same velocity as the protons. Some of these atoms decay to produce red-shifted Lα emission. Canfield and Chang (1985) have made calculations to show that this emission should be detectable above the UV continuum if a significant flux of protons is present. In view of the importance of such a result in interpreting the hard X-ray flux and understanding the flare energy release process, it is crucial that a search for such red-shifted Lα emission be made as soon as possible during the upcoming increase in solar activity.

6. Polarization

In the 1970's there were high expectations that hard X-ray polarization measurements would provide the clearest way to differentiate between thermal and nonthermal models of solar flares. Even as late as 1980, Emslie and Vlahos (1980) state that, 'hard X-ray polarization measurements are quite possibly the key to the resolution of the thermal-nonthermal-hybrid ... controversy.' Prospects for future polarization measurements are reviewed by Chanan, Emslie, and Novick (1988).

The early predictions (Bai and Ramaty, 1978) had suggested that if the electrons are

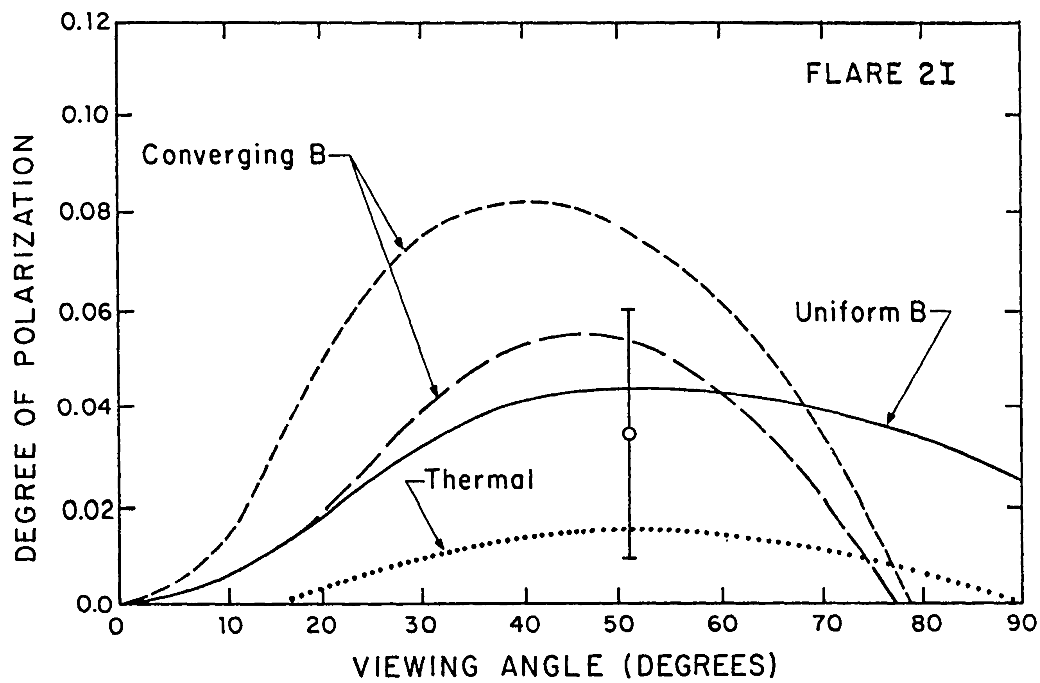

Fig. 20. Comparison of the polarization measured by Tramiel, Chanan, and Novick (1984) for an impulsive flare with the theoretical predictions of Leach, Emslie, and Petrosian (1985). The error bars shown on the data point represent $\pm 1\sigma$ uncertainties.

beamed, then the resulting X-ray emission would be highly polarized, possibly as high as 60% for limb flares, whereas if the electron velocity distribution were isotropic as in a thermal model, very little polarization ($\leq 2\%$) would be expected. Note that some residual polarization is expected even for the thermal model because of X-ray back scattering in the photosphere and the presence of temperature gradients that lead to slight electron anisotropies (Leach, Emslie, and Petrosian, 1985, and references therein).

The first measurements appeared to support the predictions of high polarization but the uncertainties were very large and the instrumentation problems severe (Tindo, Shuryghin, and Steffen, 1976; Somov and Tindo, 1978). More recent calculations taking into account electron scattering have reduced the predictions for beam models to generally $< 10\%$ (Leach and Petrosian, 1983), and new observations on the Shuttle STS-3 mission have likewise shown much lower levels of polarization (Tramiel, Chanan, and Novick, 1984). A comparison is shown in Figure 20 of the degree of polarization for one flare measured by Tramiel, Chanan, and Novick (1984) and the values predicted for different magnetic field configurations. The measured value is $3.7 \pm 2.5\%$ and applies to X-ray energies between 5 and 20 keV but predominantly below 10 keV. At these low energies there may be a considerable contribution from the relatively unpolarized thermal emission of the $< 2 \times 10^7$ K plasma. This, combined with the large error bars, makes it impossible to use the measurement to differentiate between a thermal or nonthermal model. Nevertheless, this measurement and the theoretical calculations do define the requirements for new instrumentation.

In order to make significant advances, future polarization measurements must be made at higher energies, well above the contaminating effects of the thermal emission from the $\lesssim 2 \times 10^7$ K plasma and from the 'superhot' component detected by Lin *et al.* (1981). This will require measurements at energies $\gtrsim 30$ keV. Also, detectors with higher sensitivity will be required to reduce the size of the error bars to $\lesssim 1\%$. Even with such improved polarimeters, however, the measured degree of polarization of the spatially unresolved emission may be very low and still not rule out nonthermal models. This is because of all the effects that tend to decrease the measured polarization such as Coulomb scatttering, curvature and other nonuniformity in the magnetic field, and averaging over a long time interval containing many X-ray bursts possibly from different loops. Conversely, of course, a high polarization would argue very strongly in favor of a beam model.

The best way to improve the situation would be to use an imaging polarimeter to spatially resolve the emission from different parts of a loop. In particular, the degree of polarization of the hard X-ray emission from an electron beam in the coronal part of the loop, where the density is lowest and the scattering is least, is expected to be as high as 75% for certain situations (Leach and Petrosian, 1983). Unfortunately, it is not currently feasible to build an imaging polarimeter but the coronal emission could be isolated by observing flares occurring just over the solar limb. The intensity from the upper coronal part of the loop would be a small fraction of the total emission, but given a sufficiently sensitive polarimeter that can now be built and an M- or X-class flare, it should be possible to measure the expected high degree of polarization if the electrons are even moderately beamed (Leach, Emslie, and Petrosian, 1985). Thus, the future of hard X-ray polarimetry still holds great promise even tempered by the new realism of the latest model predictions.

7. Coincident Observations at Other Wavelengths

The true potential of hard X-ray observations can only be realised when they are compared with observations at other wavelengths of the same or coincident phenomena. Among the most productive cooperative efforts have been the joint analysis of hard X-ray observations with radio, microwave, UV, soft X-ray, gamma-ray, and Hα observations. One of the frustrations has been that the other data sets have in general been obtained until recently with coarser time resolution than has been possible in hard X-rays. Since the hard X-ray emission is observed to vary on sub-second time-scales, observations at other wavelengths with this time resolution are particularly important. This general area of rapid fluctuations in solar flares was the subject of an SMM workshop by the same name (Dennis, Orwig, and Kiplinger, 1987). Some of the more important results from these coincident observations are discussed below.

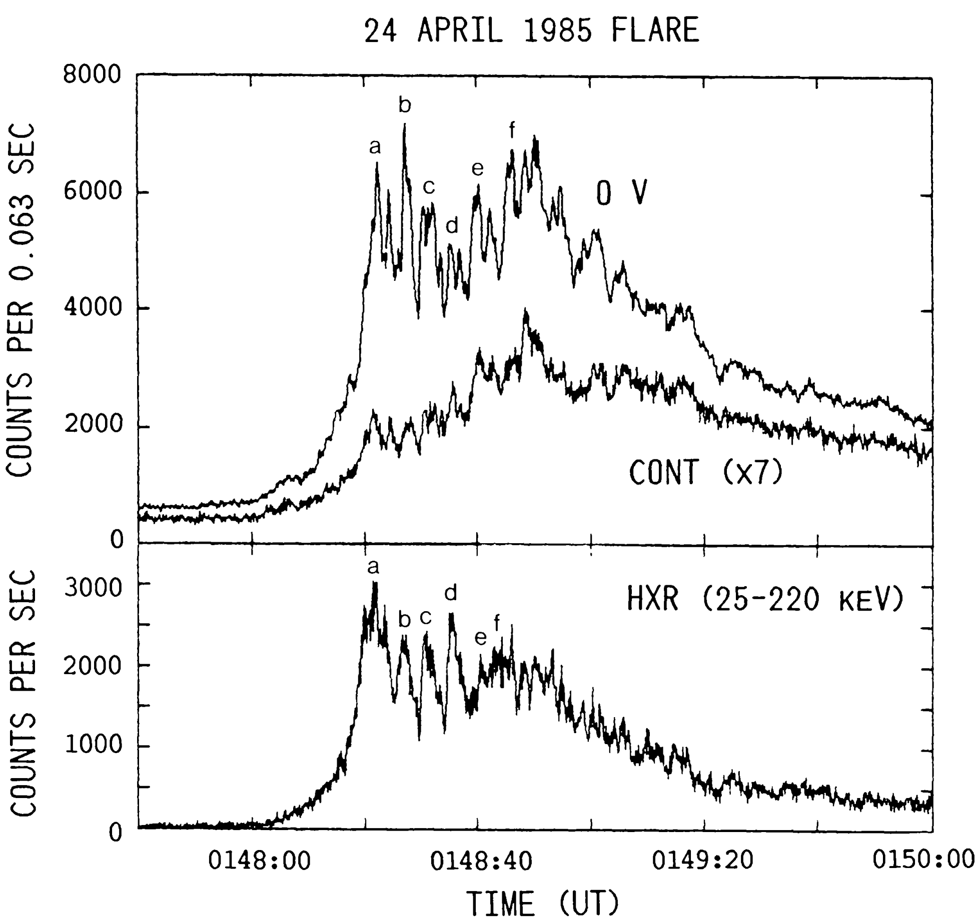

Fig. 21. Count rate vs time for the hard X-ray, O V line, and UV continuum data sets for the flare on 24 April, 1985. Small letters identify corresponding features in O V and hard X-rays (from Cheng *et al.*, 1988).

7.1. Coincident UV line and continuum observations

A comparison of hard X-ray observations with coincident, high time resolution observations of hard X-ray, ultraviolet (UV) line and continuum emissions in solar flares was reported by Orwig and Woodgate (1986). They found that in one flare on 20 May, 1984, the UV continuum and hard X-ray emissions were simultaneous to within 0.1 s. A detailed cross-correlation analysis of the three emissions in another flare on 24 April, 1985 showed that spiky features in the UV line and UV continuum emissions were simultaneous to within 0.1 s, but both UV emissions were delayed with respect to the corresponding hard X-ray features by up to 0.3 s. The time profiles of the three emissions are shown in Figure 21 and the cross-correlation coefficients are plotted in Figure 22 as functions of the lag time. Cheng *et al.* (1988) have repeated the analysis for this event and present similar results for other events. These observations place strict limitations on the energy propagation times from the corona through the transition region to the lower chromosphere during the flare impulsive phase.

The simultaneity to within 0.3 s between the hard X-ray peaks and the transition zone lines can be understood qualitatively in the electron-beam/thick-target model. However,

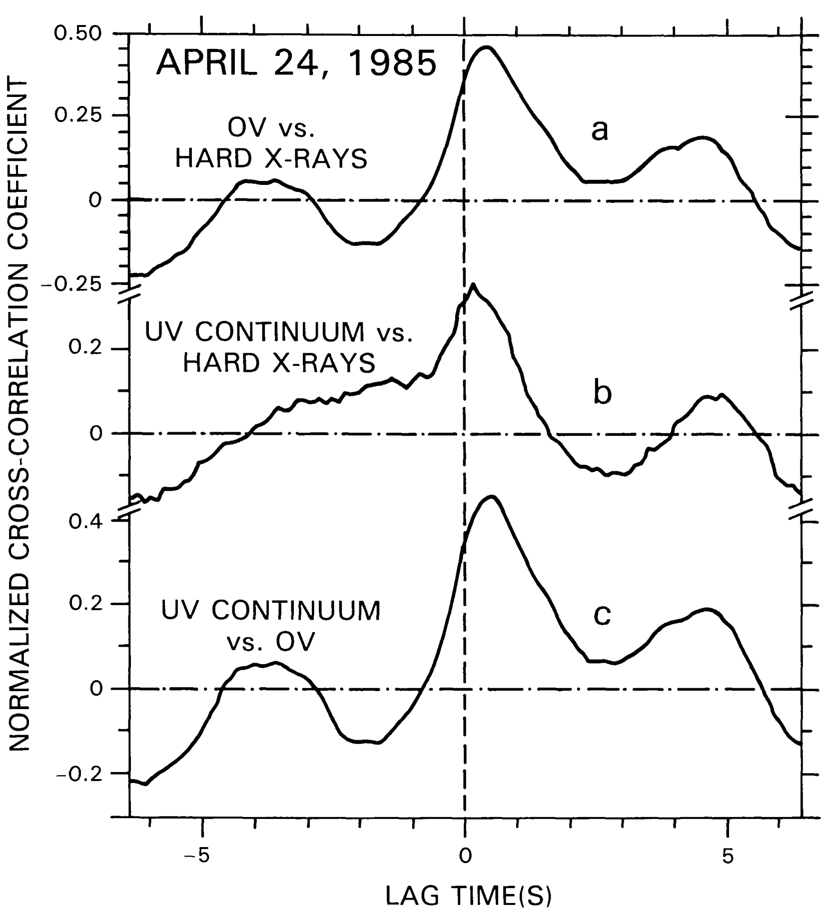

Fig. 22. Cross-correlation coefficient vs lag time for the data sets shown in Figure 21 after smoothing with a 13 s high-pass filter and subtracting the mean (from Orwig and Woodgate, 1986). Delay of (a) O v from hard X-rays, (b) UV continuum from hard X-rays, and (c) UV continuum from O v.

attempts to quantify the expected O v flux have met with limited success (see, e.g., Poland *et al.*, 1984; Emslie and Nagai, 1985; Mariska and Poland, 1985).

The simultaneity between the hard X-rays and the continuum, which is generally believed to originate from close to the temperature minimum region, is much more difficult to understand at first sight. The high-energy electrons do not make it down to this low level in the chromosphere so that direct heating is not possible. Thermal

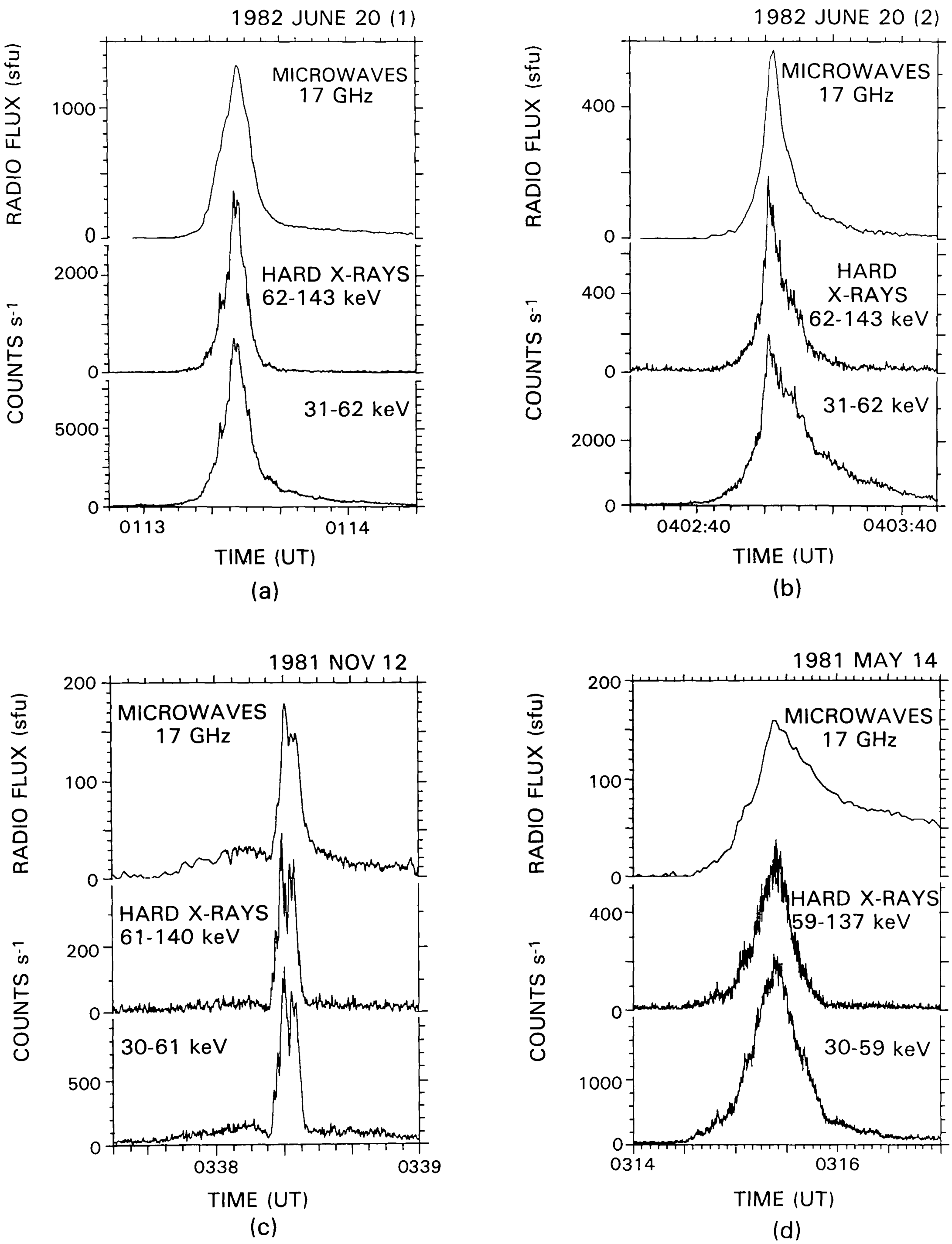

Fig. 23. Examples of simple impulsive flares showing the relationship between hard X-ray and microwave time profiles (from Kosugi, Dennis, and Kai, 1988).

conduction would take too long and is totally ineffective at these depths in any case (Emslie, Brown, and Machado, 1981). Furthermore, the extremely large energy deposition rates required at the temperature minimum region are unlikely to be attained by any canonical energy transport mechanism like accelerated particles or EUV heating (Machado and Mauas, 1987).

Machado and Mauas (1987) have suggested an alternate explanation of the observed simultaneity between the hard X-rays and UV continuum. They propose that the UV line emission from the transition region (mainly the C IV resonance line at 1549 Å) increases the amount of Si II in the temperature minimum region by the process of photo-ionization. Since the continuum emission between 1350 and 1680 Å is primarily due to electron capture by Si II (Machado and Henoux, 1982), this results in an immediate increase in the UV continuum flux. Even in the quiet Sun, Si II is produced primarily by photo-ionization rather than by collisional ionization. Increasing the density of Si II compared to that of Si I can result in an increase in the brightness temperature in the UV continuum of the magnitude observed by Orwig and Woodgate (1986) with a modest irradiation flux in the transition zone UV lines of $\sim 10^7$ erg cm^{-2} s^{-1}. This flux is to be compared to 10^{11} erg cm^{-2} s^{-1}, the flux that would be required in electrons above 20 keV in a model invoking localized heating around the temperature minimum region. While this model is attractive for its low-energy requirements and short time delay, no detailed calculations have yet been made to establish quantitative agreement with the observations.

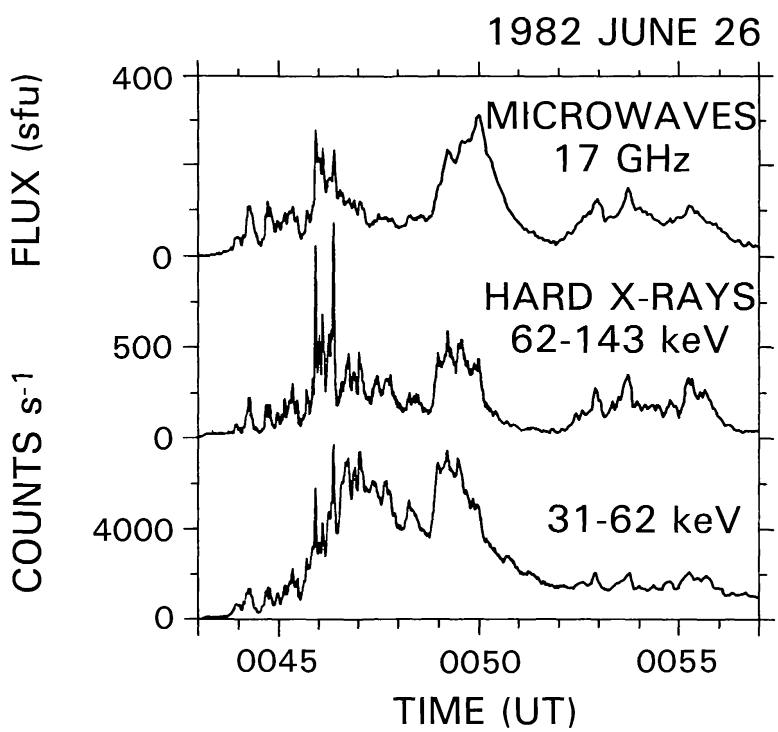

Fig. 24. A complex impulsive flare lasting for more than 10 min showing the close correlation between the hard X-ray and microwave time profile (from Kosugi, Dennis, and Kai, 1988).

7.2. Microwave – hard x-ray comparisons

It has been known since the first observation of a hard X-ray solar flare by Peterson and Winckler (1959) that the hard X-ray and the microwave time profiles are very similar to one another. Several examples of simple flares are plotted in Figure 23 and a more complex example is shown in Figure 24. Recent observations with subsecond time resolution have shown that this similarity holds on time scales of fractions of a second for impulsive flares (Kane *et al.*, 1983; Kaufman *et al.*, 1983; Cornell *et al.*, 1984; Costa, Kaufmann, and Takakura, 1984; Starr *et al.*, 1987). Individual hard X-ray and microwave spikes are in general either in coincidence or the microwave peak is delayed by a short time ranging up to a second or two. Tandberg-Hanssen *et al.* (1984) reported an unusually long delay of 6 ± 3 s. Very few cases, if any, have been observed in which the microwave emission precedes the hard X-ray emission. Much longer delays are seen in type C flares and an example is shown in Figure 25. The microwave peaks in this type of event can be delayed by as much as 10 min from the corresponding hard X-ray peaks (Cliver *et al.*, 1986b).

In addition to the good time correlation between hard X-ray and microwave bursts, there is also a good correlation between the flux levels of the two kinds of emission.

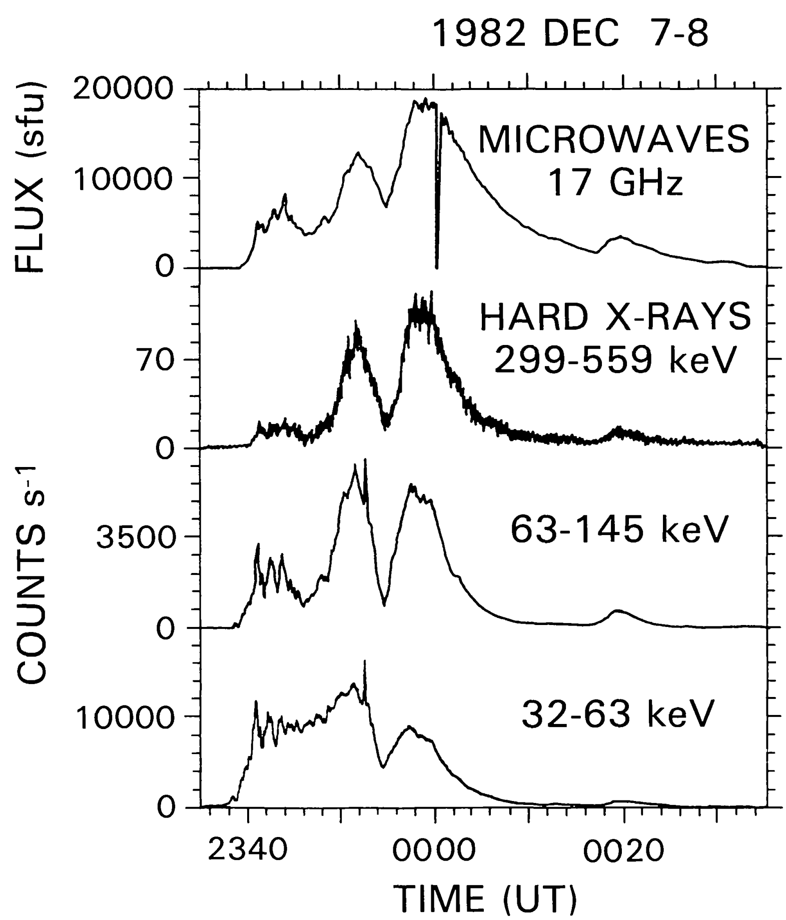

Fig. 25. An extended flare showing the evolution from a relatively spiky time structure to a more gradual variation. Note the time delay at higher X-ray energies and in 17 GHz microwaves of the last major pulse between 23:55 and 00:05 UT (from Kosugi, Dennis, and Kai, 1988).

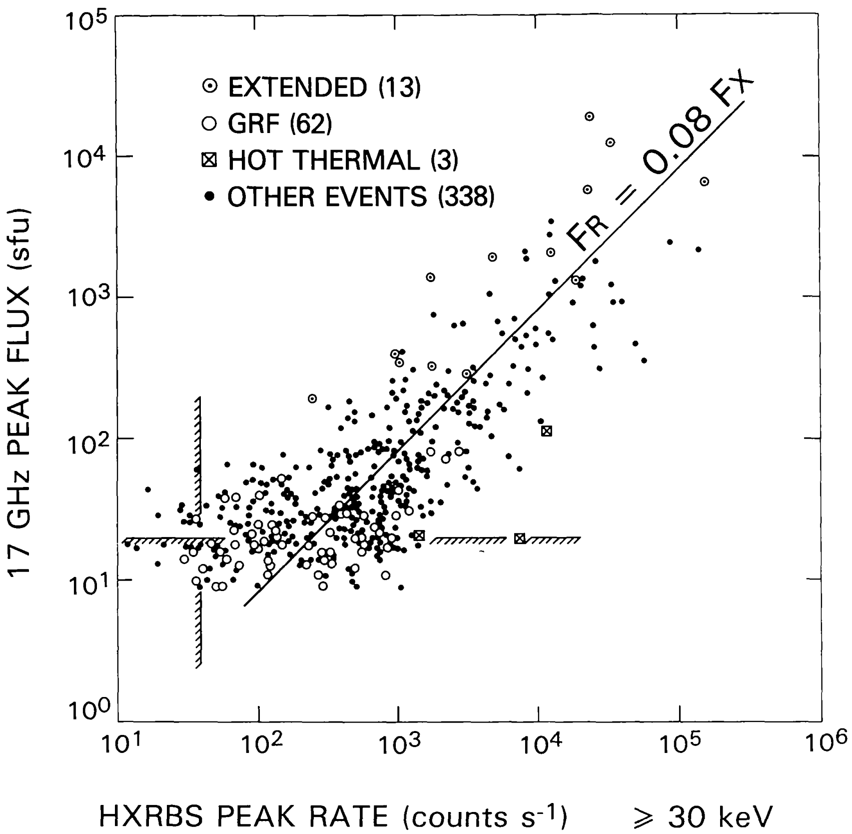

Fig. 26. Scatter plot of the Nobeyama 17 GHz peak flux versus peak X-ray count rate at energies above ~30 keV. Extended flares (⊙), flares associated with microwave gradual rise and fall (GRF) events (○), and hot thermal flares (⊠) are denoted by the special symbols indicated, with most of the others (●) being impulsive flares. The effective sensitivity thresholds of finding events are indicated by shaded lines (from Kosugi, Dennis, and Kai, 1988).

Figure 26 shows a plot of peak flux at 17 GHz vs peak hard X-ray count rate above ~30 keV for ~400 events. The scatter about the linear regression line is ~0.4 orders of magnitude RMS. Similar plots have been made by Kai, Kosugi, and Nitta (1985), Bai (1986), Cliver *et al.* (1986b).

The similarity in time profiles and the correlation of fluxes has lead many people to believe that the hard X-rays and microwaves are generated by a single population of energetic electrons accelerated in the energy release process with the hard X-rays being electron-ion bremsstrahlung and the microwaves being synchrotron radiation. Thus, the joint analysis of coincident hard X-ray and microwave observations is especially powerful since the radio emission is dependent on the magnetic field strength and direction while the hard X-ray emission is dependent on the density distribution. Many groups have attempted to exploit the potential of such comparisons but there have been many uncertainties which are only now being resolved.

7.2.1. *Electron Energies*

One of the fundamental questions concerning the microwave emission is the energy of the electrons that produce it. This cannot be determined from the microwave observations alone but an estimate can be made by comparison with the hard X-ray observations. The average energy of electrons producing hard X-rays at a given energy is well known (assuming a bremsstrahlung origin). Consequently, if the microwave emission can be associated with a given X-ray energy by detailed comparison of the time profile, then the energy of the electrons producing the microwaves can be inferred. This has been done by Nitta and Kosugi (1986), who compared the rate of flux increase at 17 GHz and at different X-ray energies, and by Kosugi, Dennis, and Kai (1988), who compared peak fluxes at 17 GHz with the peak X-ray counting rates at different energies. Both types of comparison show that for impulsive flares the energy of electrons producing the 17 GHz emission is $\lesssim 200$ keV, significantly lower than had been assumed previously. For extended flares, Kosugi *et al.* found that the energy of the electrons producing the 17 GHz emission was $\gtrsim 1$ MeV.

7.2.2. *Numbers of Electrons*

A second issue that has been a problem since Peterson and Winckler (1959) is the apparently large difference between the number of electrons that are required to produce the hard X-rays, N_x, and the number required to produce the microwaves, N_m. Early attempts to calculate N_x and N_m on the assumption that the two types of emissions were from the same population of electrons revealed a serious discrepancy for the common impulsive type B flare such that 10^3 to 10^5 more electrons were needed for the production of the X-ray burst than for the microwave burst (see Švestka, 1976 for a review). For these estimates it was assumed that the hard X-ray and microwave emissions both came from the same coronal source at densities of $\sim 10^9$ cm^{-3}. At these densities the hard X-ray emission can be determined by the thin-target approximation of Brown (1971) since collisions are infrequent and no significant evolution of the electron distribution is expected on the short, 1 s, time scales of the observations. We now know, however, based on the simultaneous observations of limb flares with two spacecraft, that the hard X-ray emission originates from low altitudes, ≤ 2500 km (Kane, 1983). Thus, it is more likely that the hard X-rays are emitted in thick-target interactions at loop footpoints, where the density may be $\geq 10^{12}$ cm^{-3}. In the thick-target approximation of Brown (1971), the electron spectrum derived from the X-ray spectrum is steeper by 1.5 in the power-law index than for the thin-target approximation. This means that N_m is lower than had previously been thought since the microwaves come from the higher energy electrons. By assuming a model in which the microwaves are produced as the electrons stream down the legs of the loop and the X-rays are produced as the same electrons stop at the footpoints, Gary (1985) and Kai (1986) were able to remove the discrepancy in the required numbers of electrons. One remaining disagreement is the required magnetic field strength; Gary (1985) used a value of 300 G whereas Kai (1986) finds that values of 500–1000 G are required.

Schmahl, Kundu, and Dennis (1985), however, were unable to entirely remove the discrepancy for a particularly well observed flare on 18 November, 1980 where the magnetic field strength and the other important parameters of the source were determined from the VLA and Berne microwave observations and the HXRBS X-ray spectrum. They found that the magnetic field was ~ 550 G. About 10^{33} electrons with an E^{-3} spectrum were required to produce the gyrosynchrotron emission whereas $\sim 10^{36}$ electrons above 25 keV with an E^{-5} spectrum were required to produce the hard X-rays. These differences can be reconciled with a thick-target model if the electrons are highly anisotropic since beamed electrons may produce a negligible microwave flux. Alternatively, the X-ray spectrum may steepen above ~ 150 keV, indicating fewer electrons at high energies to produce the microwaves. At still higher energies the electron spectrum must flatten again to be consistent with that derived from the optically-thin microwave spectrum.

Kosugi, Dennis, and Kai (1988) point out that the simple precipitation model used by Gary and Kai does not explain the microwave delay observed in some flares or the separation in position between the hard X-ray and microwave sources (e.g., Duijveman and Hoyng, 1983; Hoyng *et al.*, 1983; Kundu, 1984). To explain these observations, some form of electron trapping is required. Kosugi, Dennis, and Kai (1988) also show that the observations are not consistent with the simplest form of the thermal model in which the hard X-ray and microwave source is a common isothermal plasma.

For type C events the hard X-ray/microwave comparison is significantly different than for type B events. Figure 24 shows that these events tend to be microwave rich by a factor of up to 5 compared to type B events (Kai, Kosugi, and Nitta, 1985; Bai and Dennis, 1985; Bai, 1986). They also have a relatively low microwave peak frequency of 2–5 GHz compared to $\gtrsim 10$ GHz for the impulsive phase of these events suggesting a weaker magnetic field (Cliver *et al.*, 1986a, b; Kai *et al.*, 1986). A satisfactory model for these events is that the microwaves are emitted by MeV electrons trapped in a coronal loop or loops and the hard X-rays are produced by the same electrons according to the thin-target approximation. The magnetic field may be $\lesssim 100$ G at the loop top and much stronger in the legs of the loop leading to efficient trapping.

7.2.3. *Thermal Models*

Batchelor (1984) and Batchelor *et al.* (1985) have used joint microwave/hard X-ray observations to test their proposed modification of the Brown, Melrose, and Spicer (1979) thermal model in which a hot ($\gtrsim 10^8$ K) thermal hard X-ray source in a magnetic loop is continuously heated. The source is bounded by ion-acoustic conduction fronts which move down to the loop footpoints at the ion-sound speed given by $c_s = 9100 T_e^{1/2}$ cm s^{-1}, where T_e is the electron temperature in degrees Kelvin, i.e., $c_s = 1000$ km s^{-1} for $T_e = 1.2 \times 10^8$ K.

Batchelor *et al.* found that for twenty impulsive disk flares detected with HXRBS and with the Berne microwave antennas in 1980 and 1981, the X-ray rise time, t_r, was approximately equal to the loop length, L, divided by c_s. The appropriate value of c_s for each flare was determined from T_e derived from a thermal bremsstrahlung fit to the hard X-ray spectrum, and L was estimated from T_e and the optically-thick part of the microwave spectrum as described by Crannell *et al.* (1978). This assumes that the hard X-rays and microwaves come from the same distribution of electrons. Starr *et al.* (1988) have further extended this analysis to include six additional spike events recorded in

1980–1982. Their plot of rise time vs the theoretical time is shown in Figure 17. Note that four limb flares showed poor correlation between t_r and L/c_s, possibly because of partial occulation of the source.

MacKinnon (1985) has questioned the significance of the Batchelor *et al.* (1985) result. He finds that, for a freely expanding thermal source, the rise time is symptomatic of the time scale for primary energy release. Thus, for t_r to equal L/c_s, the energy release rate must not pass through its maximum before the source has expanded to fill the loop.

In spite of the success of the Batchelor *et al.* (1985) analysis, there is a general reluctance to accept such a thermal model. This is because other data do not support such a simple picture of a thermal source expanding from the top of the loop, although it must be remembered that this situation will only hold for the first ~ 3 to 30 s of impulsive events for loop lengths of 3000 to 30000 km, respectively. However, the thermal model ignores several observational results that seem to refute the idea that the hard X-rays and microwaves are from the same $\gtrsim 10^8$ K isothermal source.

The first discrepancy is with the hard X-ray spectrum itself, which Lin and Schwartz (1987) have shown for the one flare observed with a high resolution germanium spectrometer is not consistent with emission from an isothermal plasma. Rather they find that an acceptable fit can be obtained to a double power-law that becomes steeper at higher energies. If this is typical of impulsive flares in general, then the meaning of the 'temperature' parameter obtained from fitting a thermal-bremsstrahlung spectrum to the HXRBS observations is not clear. Note that HXRBS CsI(Na) scintillation detector has a FWHM energy resolution of about 20 keV at 30 keV, ~ 60 keV at 100 keV and ~ 190 keV at 500 keV. This should be compared to $\lesssim 1$ keV for the high-purity germanium detectors used by Lin and Schwartz.

A second similar problem is with the microwave spectrum, which Hurford has shown from high resolution observations at Owens Valley Radio Observatory (OVRO) using a frequency-agile amplifier is often more complex than that expected from an isothermal plasma (Gary and Hurford, 1986). Furthermore, simultaneous VLA observations at two widely separated frequencies – 5 and 15 GHz – have shown that the sources at these different frequencies are not always at the same position (Shevgaonkar and Kundu, 1985; Dulk, Bastion, and Kane, 1986). In these cases the flare may well consist of multiple components each with a different microwave spectrum.

Finally, the available imaging data indicate that the microwave and hard X-ray sources are generally not cospatial. Kundu (1984) reviewed simultaneous microwave and hard X-ray imaging observations of 12 bursts and found no general pattern for their locations with respect to each other although the two sources were, in general, displaced from each other. In some cases, but not all, the microwave source appeared to be located near the top of a loop with the hard X-ray source near the footpoints. It must be remembered, however, that the time resolution of the imaging observations is 10 s at best and the fundamental assumption of Batchelor *et al.* (1985) and Starr *et al.* (1988) that a common population of electrons is responsible for both the hard X-rays and microwaves only applies to the first 1 to 20 s of the flare. Consequently, a critical test of the thermal model must await imaging observations with higher time resolution.

7.3. Soft X-rays

A detailed discussion of all the implications resulting from a comparison between hard and soft X-rays is beyond the scope of this paper. The most controversial subject is the relative energies in the hard X-ray emitting electrons and the soft X-ray emitting plasma, and the possible causal relationship between the two. Also the origin of the line shifts and line broadening seen in soft X-ray emission lines during the impulsive phase and their relation to the hard X-ray emitting electrons is also the subject of ongoing controversy.

7.3.1. *The Relation between Hard and Soft X-Rays*

A commonly held belief is that the thermal source that produces the soft X-ray emission is produced, at least in part, by the high-energy electrons. This idea was first suggested by Neupert (1968), who noticed that the soft X-ray time profile often appeared as the integral of the hard X-ray profile. This connection has been questioned by Feldman, Cheng, and Doschek (1982) and Karpen, Doschek, and Seeley (1986), who suggest that there is, in fact, no causal relation between the electrons that produce the hard X-ray emission and the thermal source that produces the soft X-rays.

The essential arguments made in these two papers are given below with the counter arguments given in each case.

(1) Datlowe (1975) found that the energy content in the hard X-ray burst is not large enough to account for the soft X-ray event. This is in contradiction to Lin and Hudson (1976), Crannell, Karpen, and Thomas (1982), Antonucci, Gabriel, and Dennis (1984), and Wu *et al.* (1986), who find that, for larger events at least, the observations are consistent with the flare energy appearing initially as accelerated electrons and their subsequent energy loss producing the soft X-ray event.

(2) The soft X-ray intensity rises smoothly through the impulsive phase with no abrupt change at the time of the X-ray burst. The rate of the soft X-ray rise does tend to increase at this time, however, as evidenced by the fact that, for many events, the differential of the soft X-ray light curve shows a peak at a time close to that of the hard X-ray peak. Indeed, this is the case for the flare on 7 November 1980 presented by Karpen, Doschek, and Seeley (1986). Furthermore, Tanaka, Nitta, and Watanabe (1982) have shown excellent agreement for two impulsive events between the integral of the energy in electrons entering a thick target as derived from the hard X-ray observations and the energy in the thermal plasma as derived from the soft X-ray observations.

(3) The soft X-ray flux tends to begin before any hard X-rays are detected. This could be a sensitivity threshold problem with the hard X-ray detectors. Early in the flare when the soft X-ray emission is rising slowly, the energy input is relatively low and the expected hard X-ray flux would be very low and would possibly not show up above the background level. In addition, there could certainly be some preheating prior to the impulsive electron acceleration.

(4) The temperature of the soft X-ray emitting plasma is already near 2×10^7 K at the earliest time that the soft X-ray emission is detected and stays almost constant

during the hard X-ray burst. Emslie (1986) has further shown from data on 25 events reported by Antonucci, Gabriel, and Dennis (1984) that the maximum temperature derived from the analysis of Ca XIX line ratio is largely constant from one flare to another, independent of the hard X-ray peak rate. Emslie shows that this tendency to obtain the same value of the temperature from the Ca XIX line ratios arises because of the non-isothermal character of the flare plasma. The calculated temperature is a weighted mean value over the flare volume which tends to 'regress' towards the same value for a wide variety of possible temperature distributions. In this sense temperatures derived from line ratios are subject to the same problems as studies involving the differential emission measure distribution (Craig and Brown, 1976).

(5) The mass motions as determined from the line shifts and line broadening in soft X-rays are always near their maximum value at the flare onset and decrease thereafter. Indeed, this may be expected from the electron beam heating model since initially the density in the loop is likely to be the lowest and the electrons can reach the footpoints to produce the greatest upflow and the greatest turbulence. Later, as hot plasma rises up into the loops, the lower energy electrons can no longer reach the footpoints and the upflow and turbulence decrease.

The idea presented by Feldman, Cheng, and Doschek (1982) that the hard X-ray and soft X-ray emission are not causally related to each other seems to be a classic case of generalizing from a few pathological examples. The explanation of the apparently conflicting results may well be found in the existence of different flare types: for the impulsive type B flares, there does appear to be a good correlation and a probable causal relation between the hard and soft X-ray emissions; for type A and C flares, the correlation is certainly different and there may be no causal relation in those cases.

7.3.2. *Chromospheric Evaporation*

A related controversy is the roll of energetic electrons in driving chromospheric evaporation. Indeed, the whole concept of chromospheric evaporation itself is the subject of ongoing discussions that are summarized in Doschek *et al.* (1986), Canfield (1986), and Tanaka (1987). Recently, Zarro *et al.* (1988) have presented convincing evidence that there is momentum balance between the upflowing plasma revealed by the blue-shifted component of the Ca XIX soft X-ray emission lines and the downflowing cool gas revealed by the red-shifted component of the Hα line observed simultaneously during the impulsive phase of a small C2 flare on 30 April, 1985. This provides strong support for the explosive chromospheric evaporation model of Fisher, Canfield, and McClymont (1985a, b, c) in which beamed nonthermal electrons heat the chromosphere on a time scale shorter than the hydrodynamic expansion timescale of the heated region. This results in a large overpressure that drives hot plasma upwards into the corona and cool material downwards into the chromosphere at supersonic velocities.

Antonucci, Gabriel, and Dennis (1984) found the data to be in agreement with the chromospheric evaporation model for 25 disc flares detected with the Bent Crystal Spectrometer (BCS) on SMM and with HXRBS. (No systematic blue-shifts were found in any of the 11 flares analyzed that occurred at more than 60° from the central meridian, as expected if the blue-shift is interpreted as resulting from upflowing plasma.) In particular, they found that the increased mass energy of the coronal thermal plasma, as revealed by the unshifted Ca XIX lines, could be explained as the accumulation of the evaporated chromospheric plasma. This proposed causal connection between evaporation and the increase in the emission measure of the stationary component is strongly questioned by Karpen, Doschek, and Seeley (1986). They show that for a flare on 7 November, 1980 the calculated pressure of the evaporating material is comparable to the pressure of the plasma already in the loop. This is in contradiction with the model requirement of a high overpressure to drive the evaporation. Only by reducing the assumed footpoint area by a factor of ~ 100 could an overpressure of the magnitude required by the model be obtained. Karpen, Doschek, and Seeley conclude that for the flare under study 'the ablation process probably is not triggered (or necessarily energized) by the electrons producing the hard X-rays'.

8. Conclusions

In spite of, or in fact because of, the new and vastly improved hard X-ray observations and the coincident observations in many other wavelength bands made during the last solar cycle, the situation with regard to understanding the origin of the hard X-rays seems more obscure than ever. Even the bremsstrahlung origin from high-energy electrons has become problematic with the claim by Heristchi (1986) that the bremsstrahlung production from high-energy protons predicts only one order of magnitude more γ-rays than observed compared to the four or five orders of magnitude that had previously been computed. Simnett (1986) has also questioned the primary role of X-ray producing electrons in the flare process suggesting that protons with energies below ~ 1 MeV are produced more profusely in the energy release process. Such protons do not produce γ-ray emission as do the higher energy $\gtrsim 10$ MeV protons and resemble the Loch Ness Monster in that the evidence for their existence is highly circumstantial. They remain undetectable with current instrumentation. We must await the search for an enhanced red wing of the Lα line to determine if the number of such low-energy protons is as significant as Simnett claims.

Even if we assume that the X-ray emission is bremsstrahlung produced by high-energy electrons, the thermal/nonthermal controversy is still very much an open question although the evidence for some nonthermal emission is overwhelming for certain stages of some flares. The X-ray emission above say 100–200 keV must almost certainly be from nonthermal distributions of electrons particularly in the high-altitude type C flares. However, because of the steepness of the spectrum, the bulk of the energy in the fast electrons must be at much lower energies, below ~ 50 keV, and there the picture is much less certain.

There clearly are beams of electrons produced during the impulsive phase of many flares as revealed by the type III radio bursts but the number of electrons required to produce such a burst is several orders of magnitude below the number required to produce an X-ray burst above the threshold sensitivity of current X-ray detectors. New instruments such as the Pinhole/Occulter Facility will have sufficient sensitivity to detect such low-level X-ray emission.

The basic question is, what fraction of the total energy release during the impulsive phase is in the form of accelerated electrons and what fraction is in the form of bulk plasma heating? This question is fundamental to any attempt to determine the energy release process but it is proving to be enormously difficult to answer. Answers varying from $> 50\%$ of the energy in the form of accelerated electrons to a negligible fraction have been given based on different analyses of the same observations. Furthermore, it is not clear that future hard X-ray observations with vastly improved sensitivity, and spatial and spectral resolution will unambiguously answer the question either. Based on the current level of observations, it seems reasonable to believe that a significant fraction ($> 1\%$) of the energy released in the impulsive phase of some flares is in the form of directed beams of electrons, especially in the early stages of the impulsive phase. Smith (1985) has suggested that the energy release process changes during the impulsive phase of at least some flares, from predominantly nonthermal acceleration of electrons early in the flare to predominantly thermal heating later in the flare. Such a hybrid model is about the best that we can come up with at present.

Clearly, our best hope for resolving the thermal/nonthermal controversy is with new more sensitive and more accurate hard X-ray observations. With the next generation of instrumentation, imaging spectroscopy with sub-second time resolution and arc-second spatial resolution will be possible to allow the evolution of the electron spectrum to be determined on the temporal and spatial scales required to separate the passage of an electron beam from the expansion of a thermal source. Spectroscopy with keV energy resolution will be possible to allow the characteristic spectral slopes predicted for the different energy release processes to be clearly distinguished. Polarization measurements at the few percent level up to 100 keV will allow the highly polarized X-ray emission from electron beams in the corona to be distinguished from the essentially unpolarized emission from a thermal source, particularly for over-the-limb events where the unpolarized emission from the scattered electrons in the chromosphere is occulted. With such advanced and refined hard X-ray observations taken in conjunction with measurements at other wavelengths, we can look forward to major advances in our understanding of the flare energy release processes during the next maximum in solar activity expected to peak in 1991.

Acknowledgements

I am grateful to the many people around the world who have freely exchanged their data and ideas with me, usually in advance of publication, and who have attempted to educate me in many aspects of solar flare physics. In particular, I thank all the SMM investigators for the unique cooperation that has made this highly successful mission such a pleasure to be associated with. The SMM project including HXRBS was funded by NASA.

I thank my colleagues on the HXRBS instrument team including Ken Frost, the original PI, for their continued support and hard work. Alan Kiplinger, Richard Schwartz, and Carol Crannell offered helpful suggestions after reading an earlier version of the manuscript. Takeo Kosugi, N. Nitta, K. Kai, C.-C. Cheng, Alan Kiplinger, David Forrest, and Larry Orwig allowed me to include their results prior to publication.

The SMM observations obtained in 1984 and later were made possible by the crew of the Challenger space shuttle, who repaired the SMM spacecraft on mission 41-C. The pilot for that mission, and the commander of Challenger's last mission, was Francis R. Scobee; this paper is dedicated to his memory.

References

Antonucci, E., Gabriel, A. H., and Dennis, B. R.: 1984, *Astrophys. J.* **287**, 917.
Bai, T.: 1986, *Astrophys. J.* **308**, 912.
Bai, T. and Dennis, B. R.: *Astrophys. J.* **292**, 699.
Bai, T. and Ramaty, R.: 1978, *Astrophys. J.* **219**, 705.
Batchelor, D. A.: 1984, 'Energetic Electrons in Impulsive Solar Flares', Ph.D. Thesis, Univ. of North Carolina at Chapel Hill.
Batchelor, D. A., Crannell, C. J., Wiehl, H. J., and Magun, A.: 1985, *Astrophys. J.* **295**, 258.
Benz, A. O., Barrow, C., Dennis, B. R., Pick, M., Raoult, A., and Simnett, G. M.: 1983, *Solar Phys.* **83**, 267.
Boldt, E. and Serlemitsos, P.: 1969, *Astrophys. J.* **157**, 557.
Brown, J. C.: 1971, *Solar Phys.* **18**, 489.
Brown, J. C. and McClymont, A. N.: 1975, *Solar Phys.* **41**, 135.
Brown, J. C., Melrose, D. B., and Spicer, D. S.: 1979, *Astrophys. J.* **228**, 592.
Brown, J. C., Carlaw, V. A., Cromwell, D., and Kane, S.: 1983, *Solar Phys.* **88**, 281.
Canfield, R. C.: 1986, *Adv. Space Res.* **6**, 167.
Canfield, R. C. and Chang, C.-R.: 1985, *Astrophys. J.* **295**, 275.
Chanan, G. A., Emslie, A. G., and Novick, R.: 1988, *Solar Phys.* **118**, 309 (this issue).
Cheng, C.-C., Vanderveen, K., Orwig, L. E., and Tandberg-Hanssen, 1988, *Astrophys. J.* **330**, 480.
Cliver, E. W., Dennis, B. R., Kiplinger, A. L., Kane, S. R., Neidig, D. F., Sheeley, N. R., Jr., and Koomen, M. J.: 1986a, *Adv. Space Res.* **6**, 249.
Cliver, E. W., Dennis, B. R., Kiplinger, A. L., Kane, S. R., Neidig, D. F., Sheeley, N. R., Jr., and Koomen, M. J.: 1986b, *Astrophys. J.* **305**, 920.
Cornell, M. E., Hurford, G. J., Kiplinger, A. L., and Dennis, B. R.: 1984, *Astrophys. J.* **279**, 875.
Costa, J. E. R., Kaufmann, P., and Takakura, T.: 1984, *Solar Phys.* **94**, 369.
Craig, I. J. D. and Brown, J. C.: 1976, *Astron. Astrophys.* **59**, 239.
Crannell, C. J., Karpen, J. T., and Thomas, R.: 1982, *Astrophys. J.* **253**, 975.
Crannell, C. J., Frost, K. J., Matzler, C., Ohki, K., and Saba, J. R.: 1978, *Astrophys. J.* **223**, 620.
Crannell, C. J., Hurford, G. J., Orwig, L. E., and Prince, T. A.: 1986, *Proc. of SPIE (Large Optics Technology)* **571**, 142.
Datlowe, D. W.: 1975, in S. R. Kane (ed.), 'Solar Gamma-, X- and EUV Radiation', *IAU Symp.* **68**, 191.
De Jager, C. and Boelee, A.: 1984, *Solar Phys.* **92**, 227.
De Jager, C., Boelee, A., and Rust, D. M.: 1984, *Solar Phys.* **92**, 245.
De Jager, C. and Švestka, Z.: 1985, *Solar Phys.* **100**, 435.
De Jager, C., Machado, M. E., Schadee, A., Strong, K. T., Švestka, Z., Woodgate, B. E., and van Tend, W.: 1983, *Solar Phys.* **84**, 205.
Dennis, B. R.: 1985, *Solar Phys.* **100**, 465.
Dennis, B. R., Benz, A. O., Ranieri, M., and Simnett, G. M.: 1984, *Solar Phys.* **90**, 383.
Dennis, B. R., Frost, K. J., and Orwig, L. E.: 1981, *Astrophys. J.* **244**, L167.
Dennis, B. R., Orwig, L. E., and Kiplinger, A. L.: 1987, *Rapid Fluctuations in Solar Flares*, Workshop Proceedings, NASA CP-2449, Greenbelt, MD.
Dennis, B. R., Kiplinger, A. L., Orwig, L. E., and Frost, K. J.: 1986, in M. R. Kundu, B. Biswas, B. M. Reddy, and S. Ramadurai (eds.), *Proc. 2nd Indo-US Workshop on Solar Terrestrial Physics*, January 20–February 3, 1984, National Physical Laboratory, New Delhi, India, pp. 125–145.

Desai, U. D., Kouveliotou, C., Bara, C., Hurley, K., Niel, M., Talon, R., Vedrenne, G., Estulin, I. V., and Dolidge, V. Ch.: 1987, *Astrophys. J.* **319**, 567.

Doschek, G. A. *et al.*: 1986, in M. Kundu and B. E. Woodgate (eds.), *Energetic Phenomena on the Sun,* SMM Flare Workshop Proceedings, NASA CP-2439, Greenbelt, MD, Ch. 4.

Duijveman, A. and Hoyng, P.: 1983, *Solar Phys.* **86**, 279.

Duijveman, A., Hoyng, P., and Machado, M. E.: 1982, *Solar Phys.* **81**, 137.

Dulk, G. A., Bastian, T. S., and Kane, S.R.: 1986, *Astrophys. J.* **300**, 438.

Emslie, A. G.: 1981, *Astrophys. Letters* **22**, 171.

Emslie, A. G.: 1986, *Solar Phys.* **103**, 103.

Emslie, A. G. and Brown, J. C.: 1985, *Astrophys. J.* **295**, 648.

Emslie, A. G. and Nagai, F.: 1984, *Astrophys. J.* **279**, 896.

Emslie, A. G. and Vlahos, L.: 1980, *Astrophys. J.* **242**, 359.

Emslie, A. G., Brown, J. C., and Machado, M. E.: 1981, *Astrophys. J.* **246**, 337.

Feldman, U., Cheng, C.-C., and Doschek, G. A.: 1982, *Astrophys. J.* **255**, 320.

Fisher, G. H., Canfield, R. C., and McClymont, A. N.: 1985a, *Astrophys. J.* **289**, 414.

Fisher, G. H., Canfield, R. C., and McClymont, A. N.: 1985b, *Astrophys. J.* **289**, 425.

Fisher, G. H., Canfield, R. C., and McClymont, A. N.: 1985c, *Astrophys. J.* **289**, 434.

Forrest, D. J. and Chupp, E. L.: 1983, *Nature* **305**, 291.

Frost, K. J.: 1973, *Significant Accomplishments in Science*, NASA/GSFC, Greenbelt, MD.

Gabriel, A. H., Bely-Dubau, F., Sherman, J. C., Orwig, L. E., and Schrijver, H.: 1984, *Adv. Space Res.* **4**, 221.

Gary, D. E.: 1985, *Astrophys. J.* **297**, 799.

Gary, D. E. and Hurford, G. J.: 1986, *Bull. Am. Astron. Soc.* **18**, 900.

Harrison, R. A.: 1986, *Astron. Astrophys.* **162**, 283.

Harrison, R. A., Waggett, P. W., Bentley, R. D., Phillips, K. J. H., Bruner, M., Dryer, M., and Simnett, G. M.: 1985, *Solar Phys.* **97**, 387.

Heristchi, D.: 1986, *Astrophys. J.* **311**, 474.

Hoyng, P., Brown, J. C., and van Beek, H. F.: 1976, *Solar Phys.* **48**, 197.

Hoyng, P., Duijveman, A., Machado, M. E., Rust, D. M., Švestka, Z., Boelee, A., de Jager, C., and Frost, K. J.: 1981, *Astrophys. J.* **246**, L155.

Hoyng, P., Marsh, K., Zirin, H., and Dennis, B. R.: 1983, *Astrophys. J.* **268**, 865.

Hudson, H. S., Ohki, K. J., and Tsuneta, S.: 1985, in F. Jones, J. Adams, and G. M. Mason (eds.), *Proc. 19th Int. Cosmic Ray Conf., La Jolla,* p. 50.

Hurford, G. J. and Hudson, H. S.: 1980, 'Fourier-Transform Imaging for X-ray Astronomy', BBSO #0188, preprint, Cal. Tech., Pasadena.

Kahler, S. W. and Kreplin, R. W.: 1971, *Astrophys. J.* **168**, 531.

Kahler, S. W., Moore, R. L., Kane, S. R., and Zirin, H.: 1988, *Astrophys. J.* **328**, 824.

Kai, K.: 1986, *Solar Phys.* **104**, 235.

Kai, K., Kosugi, T., and Nitta, N.: 1985, *Publ. Astron. Soc. Japan* **37**, 155.

Kai, K., Nakajima, H., Kosugi, T., Stewart, R. T., Nelson, G. J., and Kane, S. R.: 1986, *Solar Phys.* **105**, 393.

Kane, S. R.: 1983, *Solar Phys.* **86**, 355.

Kane, S. R. and Anderson, K. A.: 1970, *Astrophys. J.* **162**, 1003.

Kane, S. R., Kai, K., Kosugi, T., Enome, S., Landecker, P. B., and McKenzie, D. L.: 1983, *Astrophys. J.* **271**, 376.

Karpen, J. T.: 1980, 'On the Origin of Multiply-Impulsive Emission from Solar Flares', PhD. Thesis, Univ. of Maryland, NASA TM82013.

Karpen, J. T., Doschek, G. A., and Seeley, J. F.: 1986, *Astrophys. J.* **30**, 327.

Kaufmann, P., Strauss, F. M., Costa, J. E. R., Dennis, B. R., Kiplinger, A. L., Frost, K. J., and Orwig, L. E.: 1983, *Solar Phys.* **84**, 311.

Kawabata, K., Ogawa, H., and Suzuki, I.: 1983, *Solar Phys.* **86**, 247.

Kiplinger, A. L.: 1987, private communication.

Kiplinger, A. L., Dennis, B. R., Frost, K. J., and Orwig, L. E.: 1982, in *Proceedings of the Hinotori Symposium on Solar Flares*, ISAS, Tokyo, Japan, pp. 66–68.

Kiplinger, A. L., Dennis, B. R., Frost, K. J., and Orwig, L. E.: 1983, *Astrophys. J.* **273**, 783.

Klein, K. L., Pick, M., Magun, A., and Dennis, B. R.: 1987, *Solar Phys.* **111**, 225.

Kosugi, T. and Kiplinger, A. L.: 1987, in B. R. Dennis, L. E. Orwig, and A. L. Kiplinger (eds.), *Rapid Fluctuations in Solar Flares*, NASA CP-2449, Greenbelt, MD, pp. 185–191.
Kosugi, T., Dennis, B. R., and Kai, K.: 1988, *Astrophys. J.* **324**, 1118.
Kundu, M.: 1984, *Adv. Space Res.* **4**, 157.
Kundu, M. and Woodgate, B.: 1986, *Energetic Phenomena on the Sun*, NASA CP-2439, Greenbelt, MD.
Leach, J. and Petrosian, V.: 1983, *Astrophys. J.* **269**, 715.
Leach, J., Emslie, A. G., and Petrosian, V.: 1985, *Solar Phys.* **96**, 331.
Lin, R. P. and Hudson, H. S.: 1976, *Solar Phys.* **50**, 153.
Lin, R. P. and Schwartz, R. A.: 1987, *Astrophys. J.* **312**, 462.
Lin, R. P., Schwartz, R. A., Pelling, R. M., and Hurley, K. C. 1981, *Astrophys. J.* **251**, L109.
Lin, H. A., Lin, R. P., and Kane, S. R.: 1985, *Solar Phys.* **99**, 263.
Lipa, B.: 1978, *Solar Phys.* **57**, 191.
Machado, M. E. and Henoux, J.-C.: 1982, *Astron. Astrophys.* **108**, 61.
Machado, M. E. and Mauas, P. J.: 1987, in B. R. Dennis, L. E. Orwig, and A. L. Kiplinger (eds.), *Rapid Fluctuations in Solar Flares*, NASA CP-2449, Greenbelt, MD, pp. 271–275.
Machado, M. E., Rovira, M. G., and Sneibrun, C.: 1985, *Solar Phys.* **99**, 189.
MacKinnon, A. L.: 1983, Ph.D. Thesis, University of Glasgow.
MacKinnon, A. L.: 1985, *Solar Phys.* **98**, 293.
MacKinnon, A. L.: 1986, *Solar Phys.* **106**, 415.
MacKinnon, A. L., Brown, J. C., and Hayward, J.: 1985, *Solar Phys.* **99**, 231.
Mariska, J. T. and Poland, A. I.: 1985, *Solar Phys.* **96**, 317.
Martens, P. C. H., Van den Oord, G. H. J., and Hoyng, P.: 1985, *Solar Phys.* **96**, 253.
McLean, D. J., Sheridan, K. V., Stewart, R. T., and Wild, J. P.: 1971, *Nature* **234**, 140.
Melozzi, M., Kundu, M. R., and Dennis, B. R.: 1988, *Astron. Astrophys.*, submitted.
Nakajima, H., Kosugi, T., Kai, K., and Enome, S.: 1983, *Nature* **305**, 292.
Neupert, W. M.: 1968, *Astrophys. J.* **153**, L59.
Nitta, N. and Kosugi, T.: 1986, *Solar Phys.* **105**, 73.
Nitta, N., Kiplinger, A. L., and Kai, K.: 1988, *Astrophys. J.*, in press.
Orrall, F. Q. and Zirker, J. B.: 1976, *Astrophys. J.* **208**, 618.
Orwig, L. E. and Woodgate, B. E.: 1986, in D. F. Neidig (ed.), *The Lower Atmosphere in Solar Flares*, Proc. NSO/SMM Symposium, 20–24 August, 1985, NSO/Sacramento Peak, Sunspot, NM, pp. 306–317.
Parks, G. K. and Winckler, J. R.: 1971, *Solar Phys.* **16**, 186.
Peterson, L. E. and Winckler, J. R.: 1959, *J. Geophys. Res.* **64**, 697.
Peterson, L. E., Datlowe, D. W., and McKenzie, D. L.: 1973, in R. Ramaty and R. G. Stone (eds.), *High Energy Phenomena on the Sun*, NASA SP-342, Greenbelt, MD, pp. 132–146.
Poland, A. I., Orwig, L. E., Mariska, J. T., Nakatsuka, R. S., and Auer, L. H.: 1984, *Astrophys. J.* **280**, 457.
Prince, T. A., Hurford, G. J., Hudson, H. S., and Crannell, C. J.: 1988, *Solar Phys.* **118**, 269 (this issue).
Raoult, A., Pick, M., Dennis, B. R., and Kane, S.: 1985, *Astrophys. J.* **299**, 1027.
Sakai, J., Nakajima, H., Zaidman, E., Tajima, T., Kosugi, T., and Brunel, F.: 1987, in B. R. Dennis, L. E. Orwig, and A. L. Kiplinger (eds.), *Rapid Fluctuations in Solar Flares*, NASA CP-2449, p. 393.
Schmahl, E. J., Kundu, M. R., and Dennis, B. R.: 1985, *Astrophys. J.* **299**, 1017.
Shevgaonkar, R. K. and Kundu, M. R.: 1985, *Astrophys. J.* **292**, 733.
Simnett, G. M.: 1986, *Solar Phys.* **106**, 165.
Simnett, G. M. and Harrison, R. A.: 1985, *Solar Phys.* **99**, 291.
Smith, D. F.: 1985, *Astrophys. J.* **288**, 801.
Somov, B. V. and Tindo, I. P.: 1978, *Cosmic Res.* **16**, 555.
Starr, R., Heindl, W. A., Crannell, C. J., Thomas, R. J., Batchelor, D. A., and Magun, A.: 1988, *Astrophys. J.* **329**, 967.
Suri, A. N., Dunphy, P. P., Chupp, E. L., and Forrest, D. J.: 1975, *Solar Phys.* **43**, 415.
Švestka, Z.: 1976, *Solar Flares*, D. Reidel Publ. Co., Dordrecht, Holland.
Švestka, Z., Schrijver, J., Somov, B., Dennis, B. R., Woodgate, B. E., Fürst, E., Hirth, W., and Klein, L.: 1983, *Solar Phys.* **85**, 313.
Tajima, T., Brunel, F., and Sakai, J.-I.: 1982, *Astrophys. J.* **258**, L45.
Tanaka, K.: 1983, in P. B. Byrne and M. Rodono (eds.), 'Activity in Red Dwarf Stars', *IAU Colloq.* **71**, 307.
Tanaka, K.: 1987, *Publ. Astron. Soc. Japan* **39**, 1.
Tanaka, K., Nitta, N., and Watanabe, T.: 1982, in *Proceedings of the Hinotori Symposium on Solar Flares*, Inst. of Space & Astronautics, Tokyo, Japan, pp. 20–26.

Tandberg-Hanssen, E., Kaufmann, P., Reichmann, E. J., Teuber, D. L., Moore, R. L., Orwig, L. E., and Zirin, H.: 1984, *Solar Phys.* **90**, 41.

Tindo, I. P., Shuryghin, A. I., and Steffen, W.: 1976, *Solar Phys.* **46**, 219.

Tramiel, L. J., Chanan, G. A., and Novick, R.: 1984, *Astrophys. J.* **280**, 440.

Tsuneta, S.: 1983, in J. C. Pecker and Y. Uchida (eds.), *Proc. of Japan–France Seminar on Active Phenomena in the Outer Atmosphere of the Sun and Stars*, CNRS and L'Observatoire de Paris, Paris, France, pp. 243–260.

Tsuneta, S., Nitta, N., Ohki, K., Takakura, T., Tanaka, K., Makishima, K., Murakami, T., and Oda, M.: 1984, *Astrophys. J.* **284**, 827.

Wild, J. P.: 1973, in R. Ramaty and R. G. Stone (eds.), *Symposium on High Energy Phenomena on the Sun*, NASA SP-342, p. 589.

Wolfson, C. J., Doyle, J. G., Leibacher, J. W., and Phillips, K. J. H.: 1983, *Astrophys. J.* **269**, 319.

Wu, S. T., de Jager, C., Dennis, B. R., Hudson, H. S., Simnett, G. M., Strong, K. T., Bentley, R. D., and Bornmann, P. L.: 1986, in M. R. Kundu and B. E. Woodgate (eds.), *Energetic Phenomena on the Sun, SMM Flare Workshop Proceedings*, NASA CP-2439, Greenbelt, MD, Ch. 5.

Yoshimori, M., Watanabe, H., and Nitta, N.: 1985a, in F. C. Jones, J. Adams, and G. M. Mason (eds.), *19th Int. Cosmic Ray Conf.*, NASA CP-2376, Greenbelt, MD, p. 54.

Yoshimori, M., Watanabe, H., and Nitta, N.: 1985b, *J. Phys. Soc. Japan* **54**, 4462.

Zaitsev, V. V. and Stepanov, A. V.: 1982, *Soviet Astron. Letters* **8**, 132.

Zaitsev, V. V., Stepanov, A. V., and Chernov, G. P.: 1984, *Solar Phys.* **93**, 363.

Zarro, D. M., Canfield, R. C., Strong, K. T., and Metcalf, T. R.: 1988, *Astrophys. J.* **324**, 582.